The Secondary Organic Aerosol Processor (SOAP v1.0) model: a unified model with different ranges of complexity based on the molecular surrogate approach

Florian Couvidat[1,2] **and Karine Sartelet**[1]

[1]CEREA, Joint Laboratory École des Ponts ParisTech/EDF R&D, Université Paris-Est, 77455 Marne-la-Vallée, France
[2]Now at Institut National de l'Environnement Industriel et des Risques, Verneuil-en-Halatte, France

Correspondence to: Florian Couvidat
(Florian.Couvidat@ineris.fr)

Abstract

The Secondary Organic Aerosol Processor (SOAP v1.0) model is presented. This model deter-
mines the partitioning of organic compounds between the gas and particle phases. It is designed
to be modular with different user options depending on the computation time and the complex-
ity required by the user. This model is based on the molecular surrogate approach, in which
each surrogate compound is associated with a molecular structure to estimate some properties
and parameters (hygroscopicity, absorption into the aqueous phase of particles, activity coeffi-
cients and phase separation).

Each surrogate can be hydrophilic (condenses only into the aqueous phase of particles), hy-
drophobic (condenses only into the organic phases of particles) or both (condenses into both
the aqueous and the organic phases of particles). Activity coefficients are computed with the
UNIFAC thermodynamic model for short-range interactions and with the AIOMFAC parame-
terization for medium and long-range interactions between electrolytes and organic compounds.
Phase separation is determined by Gibbs energy minimization.

The user can choose between an equilibrium representation and a dynamic representation of
the organic aerosol (OA). In the equilibrium representation, compounds in the particle phase are
assumed to be at equilibrium with the gas phase. However, recent studies show that the organic
aerosol is not at equilibrium with the gas phase because the organic phases could be semi-solid
(very viscous liquid phase). The condensation/evaporation of organic compounds could then be
limited by the diffusion in the organic phases due to the high viscosity. An implicit dynamic
representation of secondary organic aerosols (SOA) is available in SOAP with OA divided into
layers, the first layer being at the center of the particle (slowly reaches equilibrium) and the final
layer being near the interface with the gas phase (quickly reaches equilibrium). Although this
dynamic implicit representation is a simplified approach to model condensation/evaporation
with a low number of layers and short CPU time, it shows good agreements with an explicit
representation of condensation/evaporation (no significant differences after a few hours of con-
densation).

1 Introduction

Fine particles are regulated because of their impact on human health (WHO, 2003). Furthermore, they degrade atmospheric visibility (Larson et al., 1989) and influence climate change (Kanakidou et al., 2005). It is therefore necessary to develop models able to predict particle
[5] formation, which can be used to predict their impact on health and environment and evaluate emission mitigation policies. Particulate organic matter (OM) represents a large fraction of the total fine particulate mass, typically between 20 and 60% (Kanakidou et al., 2005; Yu et al., 2007; Zhang et al., 2007). Therefore, efforts have to be made to represent OM as accurately as possible in models. Three-dimensional (3D) air quality models, which estimate
[10] particles concentrations, need to have an implicit representation of organic species. Because of the large number of organic species involved originating from diverse anthropogenic and biogenic sources, species need to be lumped according to their properties (for example by lumping species with similar saturation vapor pressures). In the surrogate-based methodologies, molecular structures are attached to surrogate compounds representing a large number of SOA species
[15] to estimate several properties (e.g., condensation into an aqueous phase, oligomerization, hygroscopicity, non-ideality).

In 3D air quality models, several assumptions are made on the thermodynamics of OA such as equilibrium between the gas phase and the particle phase, ideality or no phase separation. However, these assumptions could strongly impact simulated OA formation. For example, some
[20] experimental recent studies emphasize the need to take into account dynamical aspects of the formation of OA rather than assuming thermodynamic equilibrium with the gas phase because OA can be highly viscous (Virtanen et al., 2010; Cappa and Wilson, 2011; Pfrang et al., 2011; Shiraiwa et al., 2011; Vaden et al., 2011; Shiraiwa and Seinfeld, 2012; Abramson et al., 2013).

Some OA models already represent the formation and the condensation of organic com-
[25] pounds using the surrogate approach: the AER/EPRI/Caltech (AEC) model (Pun et al., 2002, 2006), the Hydrophilic/Hydrophobic Organic model (H^2O) (Couvidat et al., 2012a,b) and the Model to Predict the Multiphase Partitioning of Organics (MPMPO) (Griffin et al., 2003). However, none of these models takes into account the dynamics of the condensation of organic

3

compounds, the influence of interactions between organic and inorganic compounds on activity coefficients and the phase separation of particulate organic matter into several organic phases whereas the interplay of these phenomena should be taken into account in models (Shiraiwa et al., 2013). Moreover, AEC and H_2O contrary to MPMPO assume that each compound may condense into only one phase (the organic or the aqueous phase). Computation of activity coefficients and phase separation at equilibrium has been extensively developed in the thermodynamic model AIOMFAC (Zuend et al., 2008, 2010, 2011; Zuend and Seinfeld, 2012). Shiraiwa et al. (2012) developed a multi-layer model KM-GAP which treats explicitly the condensation and particle diffusion of organic compounds as well as heat transfer and particle-phase reactions.

To represent organic aerosol formation and take into account non-ideality, phase separation and the viscous state of OA, the Secondary Organic Aerosol Processor (SOAP), destined to be implemented in 3D air quality models, is developed and presented here. This model is designed to be modular with different user options depending on the computation time and the complexity required by the user. The user can choose between an equilibrium representation and a dynamic representation of organic aerosols, between ideality and non-ideality (with or without phase separation and interactions with inorganic ions) and on which phases each surrogate compound can condense (the organic phases, the aqueous phase or all phases). This paper describes the SOAP model and the results of several test cases. As the dynamic representation of SOAP is implicit in order to work with low numbers of particle layers and short CPU times, comparisons to an explicit representation of condensation/evaporation are also presented.

2 Model development

2.1 Overview

SOAP is based on the surrogate approach in which SOA species are divided into three types: hydrophilic species (which condense only into an aqueous phase when an aqueous phase is present, i.e, when the concentration of water in aerosol is higher than 0.01 μg m^{-3}), hydropho-

4

bic species (which condense only into organic phases due to their low affinity with water) or both (condense into both phases) as chosen by the user. The model can represent the non-ideality of aerosols (interactions between organic compounds and interactions between organic and inorganic compounds represented via activity coefficients), hygroscopicity, phase separa-
5 tion and formation of SOA following an equilibrium approach or a dynamic approach.

Semi-volatile organic compounds are represented by surrogate compounds. To represent the non-ideality of aerosols, molecular structures are assigned by the user to each surrogate compound. A default structure is provided for each surrogate. This structure is used to compute the non-ideality of aerosols via activity coefficients. If the user specifies that a compound is both
10 hydrophilic and hydrophobic, the repartition between phases is done according to the value of activity coefficients. However, the user can decide that a compound is only hydrophilic or only hydrophobic (for example alkane or lowly oxidized compounds are probably not absorbed by the aqueous phase of particles). Moreover, if there is no compound that is both hydrophilic and hydrophobic, the condensation into organic phases can be solved separately from the conden-
15 sation into the aqueous phase. The system is then uncoupled. On the opposite, if there is at least one compound which is both hydrophilic and hydrophobic, the condensation into organic phases and the condensation into the aqueous phase must be solved simultaneously. The system is then coupled and consumes more CPU time. The user may prefer an uncoupled system for 3D application due to higher time efficiency.

20 To compute SOA formation, two different approaches can be used to model gas/particle partitioning: the equilibrium approach and the dynamic approach. In the equilibrium approach, aerosols are assumed to be at thermodynamic equilibrium with the gas phase. The model uses then a method of Newton-Raphson to efficiently compute the partitioning of each compound between the gas and particle phases. In the dynamic approach, condensation and particle dif-
25 fusion of organic compounds are treated with a multi-layer representation of OA (the organic mass is divided into several layers having different characteristic times to reach equilibrium). In this method, the particle size distribution is divided into sections (inside a section/bin, all particles are assumed to have the same diameter). Inside a bin, compounds condense into the aqueous phase or/and the organic phases. Furthermore, each bin can be separated into several

5

layers (the number of layers being the same for each bin) and several phases (the number of phases can change from one bin/layer to another bin/layer).

SOAP is based on the methodology of the models H^2O and AEC. However, as described above, several processes were added. The model can have species that can condense into the organic phases and the aqueous phase (like in MPMPO). It can compute the effects of the interactions between inorganic and organic compounds on the condensation of organics, phase separation of the organic aerosol, and dynamic formation of SOA. The dynamic approach developed in this study is an implicit approach to take into account particle-phase diffusion with a low number of layers and to keep a computation time as low as possible in order to be used by 3D air quality models. It does not describe particle-phase diffusion as thoroughly as KM-GAP (Shiraiwa et al., 2012).

The code can be downloaded at http://cerea.enpc.fr/en/modeles.html

2.2 Organic aerosol formation at equilibrium

The fundamental equations used in SOAP to represent the partitioning between gas and particles under the equilibrium assumption are described below.

2.2.1 Equilibrium between the gas phase and one organic phase

The equilibrium between the gas phase and one organic phase is described by Raoult's law:

$$P_i = \gamma_{i,org} X_{i,org} P_i^0 \tag{1}$$

with P_i the partial pressure of the compound i, $\gamma_{i,org}$ the activity coefficient of i in the organic phase, $X_{i,org}$ the molar fraction of i in the organic phase and P_i^0 the saturation vapor pressure of i. Pankow (1994) rewrote Eq. (1) into Eq. (2) to compute the absorption of organic compounds by an organic phase:

$$\frac{A_{p,i}}{A_{g,i}} = K_{p,i} M_o \tag{2}$$

6

with $A_{p,i}$ the concentration of i in the organic phase (in μg m^{-3}), $A_{g,i}$ the concentration of i in the gas phase (in μg m^{-3}), M_o the concentration of the organic phase (in μg m^{-3}) and $K_{p,i}$ the organic-phase partitioning coefficient (in m^3 μg^{-1}) which is computed using Eq. (3) (Pankow, 1994).

$$K_{p,i} = \frac{760 \times 8.202 \times 10^{-5} \times T}{M_{ow}\gamma_{i,org}P_i^0 \times 10^6} \tag{3}$$

with T the temperature (in K), M_{ow} the mean molar mass of the organic phase (in g/mol) and P_i^0 the saturation vapor pressure (in torr). In SOAP, activity coefficients are computed with the thermodynamic model UNIFAC (UNIversal Functional group Activity Coefficient Fredenslund et al. (1975)). Moreover, P_i^0 or partitioning constants $K_{p,i}$ are the same as those used in H^{2}O (they are generally determined by fitting to experimental results obtained in environmental chambers at a temperature T_{ref}). The partitioning coefficient is extrapolated from T_{ref} to T by using the enthalpy of vaporization ΔH_i (in J/mol) according to the Clausius-Clapeyron equation.

$$\frac{K_{p,i}(T)}{T} = \frac{K_{p,i}(T_{ref})}{T_{ref}}exp\left(\frac{\Delta H_i}{R}\left(\frac{1}{T} - \frac{1}{T_{ref}}\right)\right) \tag{4}$$

The absorption of water by the organic phase is computed with Eq. (5) derived from Eq. (1) applied for water.

$$A_{p,water} = \frac{M_{water}M_o\,RH}{\gamma_{water,org}M_{ow}} \tag{5}$$

with RH the relative humidity, M_{water} the molar mass of water (in g/mol) and $\gamma_{water,org}$ the activity coefficient of water in the organic phase.

2.2.2 Equilibrium between the gas phase and an aqueous phase

SOAP does not currently take into account the formation of inorganic aerosols. An inorganic aerosol model like ISORROPIA (Nenes et al., 1998) must be called separately and prior to the call of SOAP to provide inputs to SOAP: pH, concentrations of inorganic ions, ionic strength and the liquid water content of aerosols.

The equilibrium between the gas and aqueous phases can be described by Raoult's law (Eq. 6) but also by Henry's law (Eq. 7) if infinite dilution is assumed:

$$P_i = \gamma_{i,aq} X_{i,aq} P_i^0 \tag{6}$$

with $\gamma_{i,aq}$ the activity coefficient of i in the aqueous phase and $X_{i,aq}$ the molar fraction of i in the aqueous phase.

$$C_i = H_i P_i \tag{7}$$

with C_i the concentration (in M) of species i in the aqueous phase, P_i in atmosphere and H_i the Henry's law constant (in M/atm).

As the Henry's law is often used to express the partitioning between the gas and aqueous phases, a modified Henry's law is used to extrapolate infinite dilution conditions to all conditions using an aqueous-phase partitioning coefficient $K_{aq,i}$:

$$\frac{A_{aq,i}}{A_{g,i}} = K_{aq,i} AQ \tag{8}$$

with $A_{aq,i}$ the concentration of i in the organic phase (in $\mu g\ m^{-3}$), $A_{g,i}$ the concentration of i in the gas phase (in $\mu g\ m^{-3}$), AQ the total concentration (organics + inorganics including water) of the aqueous phase (in $\mu g\ m^{-3}$) and $K_{aq,i}$ the aqueous-phase partitioning coefficient (in $m^3/\mu g$) which is computed with Eq. (9):

$$K_{aq,i} = \frac{H_i R T}{\rho_{water} \zeta_i \times 1.013 \times 10^{11}} \times \frac{18}{M_{aq}} \tag{9}$$

with ρ_{water} the density of the aqueous phase (in $kg\ m^{-3}$), M_{aq} the molar mass of the aqueous phase (in g/mol) which can be slightly different from the molar mass of water due to the presence of other compounds and ζ_i the activity coefficient by reference to infinite dilution. ζ_i is computed with Eq. (10):

$$\zeta_i = \frac{\gamma_{i,aq}}{\gamma_{i,aq}^\infty} \tag{10}$$

8

where $\gamma_{i,aq}^{\infty}$ is the activity coefficient at infinite dilution in water, which is computed with UNIFAC. However, the original UNIFAC (Fredenslund et al., 1975) only computes the activity coefficients due to short-range interactions and does not take into account medium and long range interactions due to the presence of electrolytes in the aqueous phase. In the aqueous phase,
5 activity coefficients are computed from Eq. (11) (Zuend et al., 2008):

$$\gamma_{i,aq} = \gamma_{LR}\gamma_{MR}\gamma_{SR} \tag{11}$$

γ_{LR}, γ_{MR} and γ_{SR} are respectively the activity coefficients at long, medium and short range interactions. γ_{SR} is computed with UNIFAC whereas γ_{LR} and γ_{MR} are computed with the AIOMFAC method. The last two parameters model the influence of inorganic ions on the
10 partitioning of organic compounds (Zuend et al., 2008, 2011; Zuend and Seinfeld, 2012).

Similarly to the case of condensation into an organic phase (Eq. (4)), the partitioning coefficient is extrapolated from T_{ref} to T by using the enthalpy of vaporization ΔH_i (in J/mol) as described in Eq. (12):

$$\frac{K_{aq,i}(T)}{T} = \frac{K_{aq,i}(T_{ref})}{T_{ref}}exp(\frac{\Delta H_i}{R}(\frac{1}{T} - \frac{1}{T_{ref}})) \tag{12}$$

15 However, some compounds are acids that can dissociate in the aqueous phase. Therefore, partitioning coefficients are modified to take into account acidic dissociation as done by Pun et al. (2006).

The absorption of water by the aqueous phase is computed with Eq. (13) derived from Eq. (1):

$$A_{aq,water} = \frac{M_{water}AQ \times RH}{\gamma_{water,aq}M_{aq}} \tag{13}$$

20 with $\gamma_{water,aq}$ the activity coefficient of water in the aqueous phase. As the amount of water absorbed by inorganics is already given by the inorganic model (i.e., ISORROPIA) and is used as input of SOAP, we assumed that the total amount of water (from inorganics and organics) computed by SOAP should at least be equal to the amount of water given by the inorganic model. Therefore, if the amount of water computed by SOAP is lower than the amount computed by the
25 inorganic model, it is replaced by the amount computed by the inorganic model. This problem

9

arises because inorganics are not computed within SOAP (in that case, there would be no numerical issue) and water concentrations can be lower in SOAP than in the inorganic model ISORROPIA for several reasons. First, there can be numerical differences between SOAP and ISORROPIA because different parameterizations are used in SOAP and ISORROPIA to
5 compute water concentrations: SOAP computes the amount of water using the water activity computed by the thermodynamic models UNIFAC and AIOMFAC whereas ISORROPIA computes the amount of water using the ZSR correlation (Robinson and Stokes, 1965). Second, the amount of water absorbed by the aerosol can be different from the sum of the water amount absorbed by inorganics and the water amount absorbed by organics. Choi and Chan (2002)
10 found that organic species can either reduce or enhance the water absorption of inorganic compounds. Depending on the conditions, the amount of water computed by SOAP could be higher without organics than with. We chose here to assume that the amount of water should at least be equal to the amount of water given by ISORROPIA, although it would be possible to keep the amount of water computed by SOAP even when lower than the amount of water computed
15 by ISORROPIA. However, if the amount of water given by SOAP is significantly lower than ISORROPIA, this would induce changes in the amount of inorganics in the aerosol. As the amount of inorganics may not be recomputed after SOAP, we considered that amount of water is at least equal to the amount of water given by ISORROPIA, the amount of water being recomputed only to provide a better estimate of the amount of water when water absorption
20 are mainly due to organics. The best way to deal with this dilemma would be to fully couple inorganic and organic aerosol formation.

2.2.3 Equilibrium between the gas phase and several particulate phases

SOAP can compute the partitioning of compounds between the gas phase and several particulate phases. The user can specify for each compound if it is hydrophilic (condense into the
25 aqueous phase of particles) or hydrophobic (condense into the organic phase of particles) or both hydrophilic and hydrophobic (condense into both phases).
For an uncoupled system (compounds cannot be both hydrophobic and hydrophilic), for hy-

10

drophobic compounds, the total concentration of i in all phases $A_{tot,i}$ is:

$$A_{tot,i} = A_{p,i} + A_{g,i} \tag{14}$$

which gives when combined to Eq. (2):

$$A_{p,i} = A_{tot,i} \frac{K_{p,i} M_o}{1 + K_{p,i} M_o} \tag{15}$$

A method of Newton-Raphson is then used to solve Eq. (15) and to minimize the error (an accuracy threshold is provided by the user):

$$error = M_o - \sum_i A_{tot,i} \frac{K_{p,i} M_o}{1 + K_{p,i} M_o} \tag{16}$$

For an uncoupled system, for hydrophilic compounds, the total concentration of i in all phases $A_{tot,i}$ is:

$$A_{tot,i} = A_{aq,i} + A_{g,i} \tag{17}$$

which gives if combined to Eq. (8):

$$A_{aq,i} = A_{tot,i} \frac{K_{aq,i} AQ}{1 + K_{aq,i} AQ} \tag{18}$$

A method of Newton-Raphson is then used to solve Eq. (18) and to minimize the error (an accuracy threshold is provided by the user):

$$error = AQ - AQ_{inorg} - \sum_i A_{tot,i} \frac{K_{aq,i} AQ}{1 + K_{aq,i} AQ} \tag{19}$$

with AQ_{inorg} the concentration of inorganic compounds in the aqueous phase. For a coupled system, the total concentration of i in all phases $A_{tot,i}$ is:

$$A_{tot,i} = A_{p,i} + A_{aq,i} + A_{g,i} \tag{20}$$

11

which gives if combined to Eq. (2) and (8):

$$A_{p,i} = A_{tot,i} \frac{K_{p,i} M_o}{1 + K_{aq,i} AQ + K_{p,i} M_o} \tag{21}$$

$$A_{aq,i} = A_{tot,i} \frac{K_{aq,i} AQ}{1 + K_{aq,i} AQ + K_{p,i} M_o} \tag{22}$$

Similarly, a method of Newton-Raphson is used to solve simultaneously Eq. (21) and (22) and to minimize the errors ($error1_p$ and $error_{aq}$).

$$error_p = M_o - \sum_i A_{tot,i} \frac{K_{p,i} M_o}{1 + K_{aq,i} AQ + K_{p,i} M_o} \tag{23}$$

$$error_{aq} = AQ - AQ_{inorg} - \sum_i A_{tot,i} \frac{K_{aq,i} AQ}{1 + K_{aq,i} AQ + K_{p,i} M_o} \tag{24}$$

2.2.4 Saturation and separation of organic phases

If compounds having a low affinity with each other coexist inside a single organic phase, the organic phase may become saturated by some compounds and may become unstable. In that case, the separation of the organic phase into several organic phases (having different composition) may occur. To determine whether separating the organic phase into several organic phases makes the system more stable, the Gibbs energy G is computed as in Erdakos and Pankow (2004); Zuend et al. (2010); Zuend and Seinfeld (2012) using different system configurations (different number of phases):

$$G = \sum_i \sum_\phi n_i^\phi \mu_i^\phi \tag{25}$$

with ϕ an index of the various phases (gaseous and liquid), n_i^ϕ the number of moles of species i in phase ϕ and μ_i^ϕ the chemical potential of i in phase ϕ.

The most stable configuration of the system has the lowest Gibbs energy. Therefore, if by

12

adding one organic phase the Gibbs energy decreases, then the system is more stable and phase separation takes place. If the Gibbs energy does not decrease, the previous solution (before adding one organic phase) is more stable and is kept. The number of organic phases is determined iteratively: one phase is added until the Gibbs energy increases.

The partitioning of organic compounds into an aerosol with several organic phases are determined with equations 21 and 22 generalized to several organic phases:

$$A_{p,i}^{phase} = A_{tot,i} \frac{K_{p,i}^{phase} M_o^{phase}}{1 + K_{aq,i} AQ + \sum_{\phi} K_{p,i}^{\phi} M_o^{\phi}} \tag{26}$$

$$A_{aq,i} = A_{tot,i} \frac{K_{aq,i} AQ}{1 + K_{aq,i} AQ + \sum_{\phi} K_{p,i}^{\phi} M_o^{\phi}} \tag{27}$$

2.3 Dynamic gas uptake by organic particles

The dynamic approach, which is presented hereafter, is an implicit representation to take into account particle-phase diffusion with a low number of layers, and have a computation time as low as possible to be used in 3D air quality models. The main assumptions are described here.

The first assumption is that the organic-phase diffusion coefficient is constant over the entire particle. It does not depend on the distance to the center of the particle. Although this assumption may not be valid, it is reasonable because, currently, to our knowledge, there is no parameterization to evaluate the order of magnitude of organic-phase diffusion coefficients.

The second assumption is that in the model there is no direct exchange of compounds between layers and that the compounds condense directly from the gas phase to the layer or that they evaporate directly from the layer to the gas phase by taking into account an equilibration time specific of the layer. Compounds condense into a layer or evaporate from a layer as if the other layers had the same affinity with compounds. Effects of entrapment of compounds inside central layers by the layers closer to the gas-phase interface (compounds inside the central layers having a low affinity with the compounds of the layers at the interface will not be able to evaporate whereas compounds having a high affinity with the central layer but having a low

13

affinity with the layers at the interface will not be able to condense into the central layer) are not taken into account. The model should give however a good estimation of the capacity of the organic aerosol to absorb compounds (by taking into account the time for each layer to reach equilibrium due to diffusion in the particle).

The third assumption is that the organic phases and the aqueous phase evolve separately, i.e., there is no kinetic transfer of compounds between the organic phases and the aqueous phase, due to the complexity of representing properly those transfers, which should strongly depend on the morphology of particles. If a compound tends to go from the aqueous phase to the organic phases, it has first to go from the aqueous phase to the gas phase and then from the gas phase to the organic phases. For example, in case of evaporation of the aqueous phase (that can be due to a strong change of the relative humidity), this assumption can create some evaporation/recondensation issue in the model (compounds evaporate and recondense after some time into the organic phases according to condensation/evaporation fluxes). Actually, a part of organic compounds should go directly from the aqueous phase to the organic phases. It could also be possible that if an aqueous phase coexists with organic phases into the same particle that organic compounds do not condense directly from the gas phase into the organic phases (because the kinetic is too slow) but condense first into the aqueous phase and then go from the aqueous phase to the organic phases (if it is quicker for a compound to condense into the organic phases by this pathway). However, it can also be argued that if there is an aqueous phase (the relative humidity is high), the organic phases may not be significantly viscous and therefore high organic-phase diffusion coefficient should be used.

Finally, the model assumes that there is no gradient of the gas-phase concentrations near the interface with the particle. If the particle is divided into two separated regions (one aqueous and one organic), an angular gradient of gas-phase concentrations could influence the condensation of compounds into the two regions. To address properly this phenomenon, the particle and the gas phase at the vicinity of the particle should be discretized as a function of the angular gradient. However, due to the high diffusivity of organic compounds in the gas phase, the diffusion of organic compounds around the particle should be very fast compared to the kinetic of condensation and therefore, this assumption should have a low effect on condensation/evaporation.

14

2.3.1 Diffusion of organic compounds in spherical organic particles

The diffusion of organic compounds at a radius r at time t inside a spherical particle is governed by the following Eq. (Seinfeld and Pandis, 1998):

$$\frac{\partial C}{\partial t} = D_{org}\left(\frac{\partial^2 C}{\partial r^2} + \frac{2}{r}\frac{\partial C}{\partial r}\right) + R_{org}(r,t) \tag{28}$$

with C(r,t) the molar concentration at radius r at time t, D_{org} the organic-phase diffusivity and R_{org} the organic-phase reaction rate. By assuming D_{org} constant, the solution of this equation (with C(r,0)=0 and C(R_p,t)= C_s, R_p being the radius of the particle) without organic-phase reaction is according to Seinfeld and Pandis (1998):

$$\frac{C(r,t)}{C_s} = 1 + \frac{R_p}{r}\sum_{n=1}^{\infty}(-1)^n\frac{2}{n\pi}sin\frac{n\pi r}{R_p}exp\left(-\frac{n^2\pi^2 D_{org}\,t}{R_p^2}\right) \tag{29}$$

By integrating Eq. (29) over the volume of a spherical particle, the following equation is found for the concentration in the particle phase A_p:

$$\frac{A_p(t)}{A_{eq}} = 1 - \sum_{n=1}^{\infty}\frac{6}{n^2\pi^2}exp\left(-\frac{n^2\,t}{\tau_{dif}}\right) \tag{30}$$

with τ_{dif} the characteristic time for diffusion in the center of the particle:

$$\tau_{dif} = \frac{R_p^2}{\pi^2 D_{org}} \tag{31}$$

with A_{eq} the organic phase concentration at equilibrium with the gas phase (A_{eq}=$K_p M_o A_g$). In Eq. (30), A_p can be interpreted as the sum of an infinity number of layers of concentration A_p^{layer}:

$$A_p = \sum_{layer=1}^{\infty} A_p^{layer} \tag{32}$$

$$A_p^{layer} = V_{layer} A_{eq} \left(1 - exp \left(-\frac{\alpha_{layer}\, t}{\tau_{dif}} \right) \right) \tag{33}$$

where A_p^{layer} is the concentration (in μg/m^3) in a layer of volume fraction V_{layer} determined by the fraction of the volume of the particle constituted by the layer and α_{layer} the ratio between the characteristic diffusion time at the center of the particle τ_{dif} to the characteristic diffusion time τ_{dif}^{layer} of the layer such as:

$$\alpha_{layer} = \tau_{dif}/\tau_{dif}^{layer} \tag{34}$$

Numerically, Eq. (30) can be approached by a finite number of diffusion layers N_{layer}^{dif} (number of layers into which diffusion occurs) and by fitting the parameters V_{layer} and α_{layer} such as:

$$A_p = \sum_{layer=1}^{N_{layer}^{dif}} A_p^{layer} \tag{35}$$

First, for a given concentration A_{eq}, a given D_{org}, R_p, we estimate $A_p(t)$ using Eq. (32). Then V_1, V_2, V_3, α_1, α_2, α_3 are fitted such as satisfying Eq. (35). The values of these parameters do not depend of the choice of A_{eq}, D_{org} and R_p.

For example, if we choose to have 3 diffusion layers, then V_1=0.6, V_2=0.26, V_3=0.14, α_1= 0.9878, α_2=6.2558, α_3=68.8666. For 4 diffusion layers, we use V_1=0.608, V_2=0.218, V_3=0.121, V_4=0.053, α_1=0.998, α_2=4.904, α_3=30.98, α_4=663.4. Eq. (35) gives a good approximation of Eq. (32) as shown in Fig. 1 with 3 and 4 diffusion layers although with 3 diffusion layers, diffusion is underestimated for low concentrations (lower than one tenth of the concentration at equilibrium).

The evolution of concentrations $A_{p,i}^{bin,layer}$ in a bin and a layer due to the condensation of species i limited by the diffusion of organic compounds in the organic phase is described by the Eq. (36), which describes the flux of diffusion $J_{diff,i}^{bin,layer}$, i.e. the evolution of the concentration $A_{p,i}^{bin,layer}$ compared to an equilibrium concentration (Pankow model: $A_{eq}^{bin,layer}$=$A_{g,i}$

16

$K_{p,i}^{bin,layer} M_o^{bin,layer}$) (with the assumption that the concentrations in one layer can be described independently from the concentrations in the other layers).

$$J_{diff,i}^{bin,layer} = \frac{dA_{p,i}^{bin,layer}}{dt} = k_{diffusion}(A_{g,i} K_{p,i}^{bin,layer} M_o^{bin,layer} - A_{p,i}^{bin,layer}) \tag{36}$$

with $M_o^{bin,layer}$ the total mass of the organic phase in the layer computed with Eq. (37) by assuming that the density of the organic matter is constant over layers and $k_{diffusion}$ the kinetic coefficient for diffusion (in s^{-1}) computed with Eq. (38) as the inverse for the characteristic diffusion time in a layer.

$$M_o^{bin,layer} = V_{layer} M_o^{bin} \tag{37}$$

$$k_{diffusion} = \frac{\alpha_{layer}}{\tau_{dif}} \tag{38}$$

2.3.2 Diffusion of organic compounds in more complex particles

The previous equations correspond to the diffusion of organic compounds into an entirely organic spherical particle. However in the atmosphere, particles generally have more complex geometries and can also be constituted by solid and/or inorganic phases. The morphology affects the time for an organic phase to be diffused in the particle. For example, for a same particle diameter, a particle entirely organic needs more time to reach equilibrium with the gas phase than a particle constituted by a solid core in the center surrounded by an organic phase (because the organic compounds do not penetrate the particle all the way to the center, they are only diffused inside the coating). As diffusion of organic compounds is affected by the presence of solid phases, morphology factors are designed to take into account this solid phase where diffusion of organics may not occur. We assume that this solid phase is located at the core of particles based on Katrinak et al. (1993); Sachdeva and Attri (2007); Wang et al. (2014). Models, such as KM-GAP, treating explicitly the diffusion of compounds inside particles do not need those factors. As in SOAP, the volume of layer has to be constant, only the characteristic time for diffusion can be affected by the morphology. We propose here to parameterize the effects of a

17

solid core by defining morphology factors f_{morph}^{layer}, which affect the time to reach equilibrium with the gas phase. The characteristic time for diffusion of a layer τ_{dif}^{layer} expressed in Eq. (34) becomes:

$$\tau_{dif}^{layer} = \frac{\tau_{dif}}{f_{morph}^{layer}\alpha_{layer}} \tag{39}$$

5 Eq. (36) then becomes:

$$J_{diff,i}^{bin,layer} = \frac{dA_{p,i}^{bin,layer}}{dt} = f_{morph}^{layer}k_{diffusion}(A_{g,i}K_{p,i}^{bin,layer}M_o^{bin,layer} - A_{p,i}^{bin,layer}) \tag{40}$$

with $k_{diffusion}$ defined as in Eq. (38).

The morphology factors can be determined numerically (at least for some simple case). We determined here morphology factors in the case of a spherical particle with a solid core at the center of the particle. The differential equation for diffusion (Eq. 28) is solved and morphology factors are fitted to minimize the differences between Eq. (28) and (40) for various volume fractions of the solid phase f_s (volume of the solid phase in the particle over the volume of the particle). This fitting procedure is described into more details in the supplementary materials. The variations of the morphology factors with the volume fraction f_s are shown in Fig. 2 for 3 and 4 diffusion layers. The morphology factors for a solid core particle can be represented by a polynomial expression such as:

$$f_{morph}^{layer} = A_{layer}f_s^4 + B_{layer}f_s^3 + C_{layer}f_s^2 + D_{layer}f_s + 1 \tag{41}$$

The values of the polynomial parameters are shown in Table 2. Typically, the presence of a solid phase would result in a morphology factor greater than 1, reducing the characteristic diffusion time of organics in the particle. This parameterization only takes into account the simple case of a spherical solid core at the center and not the wide range of morphologies present in the atmosphere. A similar methodology or a methodology based on observations could be applied to other morphologies which could greatly affect the characteristic times for diffusion. For example, morphology factors for the effect of the presence of an aqueous phase on characteristic

18

time for diffusion could be determined (at least as a function of the mass of the aqueous phase and the affinity of compounds with water). Currently, the model assumes there is no effect of the aqueous phase on the characteristic times.

2.3.3 Condensation/evaporation of organic compounds into a viscous particle

In this part, the methodology to compute condensation/evaporation/diffusion inside a viscous particle is described. The algorithm to compute condensation/evaporation/diffusion fluxes is divided into two steps shown in Figures 3 and 4. In the first step, the total flux of condensation/evaporation/diffusion over the whole particle is computed whereas in the second step, this flux is redistributed among layers. The complete methodology to compute fluxes is described hereafter.

The evolution equation of concentration of species i by diffusion in each bin and layer is described by Eq. (40). To properly take into account the condensation/evaporation of low volatile compounds, a thin surface layer, which is not limited by diffusion, is added to the model. In case of very low diffusivity, this layer allows non-volatile and low volatility compounds to condense at the surface of particles without any limitation due to diffusion. Let us denote N_{layer} the number of layer into which the dynamic of condensation/evaporation/diffusion is solved. We have:

$$N_{layer} = N_{layer}^{diff} + 1 \tag{42}$$

A volume fraction V_{layer} for the interface layer of 0.01 is used (using a lower volume fraction does not change significantly the results). Adding an interface layer between the gas and the particle slightly reduces the volume of the other layers, as described in section 2.3.1. In this paper, simulations are performed with 4 layers (3 diffusion layers: V_1=0.6, V_2=0.26, V_3=0.13 and V_4=0.01) and with 5 layers (4 diffusion layers: V_1=0.608, V_2=0.218, V_3=0.121, V_4=0.043 and V_5=0.01).
The flux of diffusion in the upper layer (the interface) is zero, as diffusion should not limit

19

absorption at the interface:

$$J_{diff}^{bin,interface} = 0 \tag{43}$$

The evolution of concentrations by condensation/evaporation at the interface, i.e. the flux of condensation/evaporation at the interface, is:

$$J_i^{bin,interface} = k_{absorption} \left(A_{g,i} - A_{g,i}^{eq,bin,interface} \right) \tag{44}$$

with $A_{g,i}^{eq,bin,interface}$ the gas-phase concentration at equilibrium with the interface layer and $k_{absorption}$ the kinetic rate of absorption, which is (Seinfeld and Pandis, 1998):

$$k_{absorption} = 2\pi D_p D_{air} N^{bin} f(Kn,\alpha) \tag{45}$$

with D_p the diameter of the particle, D_{air} the diffusivity of compound i in air, $f(Kn,\alpha)$ the transition regime formula of Fuchs and Sutugin (1971).

The gas-phase concentration at equilibrium with the interface layer $A_{g,i}^{eq,bin,interface}$ is computed as follows:

$$A_{g,i}^{eq,bin,interface} = K_{effect} \frac{A_{p,i}^{bin,interface}}{K_{p,i}^{bin,interface} M_o^{bin,interface}} \tag{46}$$

with $K_{p,i}^{bin,interface}$ the partitioning coefficient into the interface layer for compound i and $M_o^{bin,interface}$ the total organic mass concentrations of the interface layer and K_{effect} the Kelvin effect correction coefficient:

$$K_{effect} = exp\left(-\frac{2\sigma M_{ow}^{bin}}{RT\rho_{organic}} \right) \tag{47}$$

with σ the surface tension, $\rho_{organic}$ the density of the organic phase, M_{ow} the mean molar mass of the organic phase at the surface of the particle (molar mass of the layer at the interface) and R_p the radius of the particle. A surface tension of 24 mN/m is chosen, which is roughly the surface tension of organic compounds according to Seinfeld and Pandis (1998) and a density of the organic phase of 1300 kg/m^3 is used.

In a comprehensive dynamic model, diffusion would be represented explicitly. However, to have

20

a model with a low number of layers and gain CPU time, the evolution of the concentrations in each layer is solved by considering the combined effect of condensation/evaporation and diffusion in the particle. The flux of condensation/evaporation/diffusion of a compound i inside a bin and a layer is noted $J_{tot,i}^{bin,layer}$ and is used to compute the evolution of concentrations of a compound i inside a layer:

$$\frac{dA_{p,i}^{bin,layer}}{dt} = J_{tot,i}^{bin,layer} \tag{48}$$

The evolution of the total mass of the particle $J_{tot,i}^{bin}$ can be computed by assuming that the characteristic time of the combined effect of condensation/evaporation and diffusion is equal to the sum of the characteristic times of condensation/evaporation and diffusion:

$$\frac{1}{J_{tot,i}^{bin}} = \frac{1}{J_{cond/evap,i}^{bin}} + \frac{1}{J_{diff,i}^{bin}} \tag{49}$$

where $J_{cond/evap,i}^{bin}$ is the flux limited by condensation/evaporation and $J_{diff,i}^{bin}$ the flux limited by diffusion. $J_{diff,i}^{bin}$ is the sum of the diffusion fluxes over all bins (each of them being computed by equation (40)):

$$J_{diff,i}^{bin} = \sum_{layer}^{N_{layer}} J_{diff,i}^{bin,layer} \tag{50}$$

$J_{cond/evap,i}^{bin}$ is obtained similarly to the interface flux of condensation/evaporation

$$J_{cond/evap,i}^{bin} = k_{absorption} \left(A_{g,i} - A_{g,i}^{eq,bin} \right) \tag{51}$$

with $A_{g,i}^{eq,bin}$ the gas phase concentration at equilibrium with the whole particle.

The gas-phase concentration at equilibrium with the particle is assumed to correspond to the sum of the gas-phase concentrations at equilibrium with each layer weighted by their kinetic of diffusion:

$$A_{g,i}^{eq,bin} = \sum_{layer}^{N_{layer}} f_i^{bin,layer} A_{g,i}^{eq,bin,layer} \tag{52}$$

21

with $A_{g,i}^{eq,bin,layer}$ the gas-phase concentration at equilibrium with the layer and with $f_i^{bin,layer}$ a weighting factor that depends on the kinetic of diffusion.

$$A_{g,i}^{eq,bin,layer} = K_{effect} \frac{A_{p,i}^{bin,layer}}{K_{p,i}^{bin,layer} M_o^{bin,layer}} \tag{53}$$

with K_{effect} the Kelvin effect correction coefficient computed with Eq. (47).

The coefficient $f_i^{bin,layer}$ corresponds to the fraction of the compound i that arrives by diffusion in the layer if compound i condenses or the fraction of the compound i that departs from the layer if the compound i evaporates. The weighting factor is computed with the following algorithm, which separates positive fluxes from negative fluxes. In case of condensation of a compound i ($J_{tot,i}^{bin} > 0$), the compound condenses preferentially on layers with positive diffusion fluxes $J_{diff,i}^{bin,layer}$. Therefore, if $J_{diff,i}^{bin,layer}$ is negative inside a layer, this layer is not taken into account in the condensation flux. On the opposite, in case of evaporation of a compound i ($J_{tot,i}^{bin} < 0$), the compound evaporates from layers with negative $J_{diff,i}^{bin,layer}$. In other words, $f_i^{bin,layer}$ is computed by weighting the diffusion fluxes $J_{diff,i}^{bin,layer}$ depending on their signs.

$$f_i^{bin,layer} = \frac{J_i^{bin,layer}}{\sum_{layer}^{N_{layer}} J_i^{bin,layer}} \tag{54}$$

with $J_i^{bin,layer}$ a flux that depends on the diffusion flux sign in each layer:

If the flux of diffusion of compound i into the particle is positive ($J_{diff,i}^{bin} > 0$):

with for the interface layer $J_i^{bin,layer} = J_i^{bin,interface}$ if $J_i^{bin,interface} > 0$ else $J_i^{bin,layer} = 0$

and for other layers $J_i^{bin,layer} = J_{diff,i}^{bin,layer}$ if $J_{diff,i}^{bin,layer} > 0$ else $J_i^{bin,layer} = 0$

If the flux of diffusion of compound i into the particle is negative ($J_{diff,i}^{bin} < 0$):

with for the interface layer $J_i^{bin,layer} = J_i^{bin,interface}$ if $J_i^{bin,interface} < 0$ else $J_i^{bin,layer} = 0$

and for other layers $J_i^{bin,layer} = J_{diff,i}^{bin,layer}$ if $J_{diff,i}^{bin,layer} < 0$ else $J_i^{bin,layer} = 0$

$$(55)$$

Once the weighting factors are computed, the flux of condensation/evaporation/diffusion over all layers $J_{tot,i}^{bin}$ can be computed with Eq. (49) to (51). These weighting factors are used to redistribute the gas-phase concentration at equilibrium between layers from a "bulk" gas-phase concentration (Eq. (52)), but also to redistribute the total flux of condensation/evaporation/diffusion between layers from the "bulk" total flux of condensation/evaporation/diffusion. The computation of the total flux per layer $J_{tot,i}^{bin,layer}$ is now explained. The total flux of condensation/evaporation/diffusion $J_{tot,i}^{bin}$ is separated into three fluxes J_i^+ (equal to the sum of diffusion fluxes which are positive), J_i^- (equal to the sum of diffusion fluxes which are negative) and the flux at the interface $J_i^{bin,interface}$:

$$J_{tot,i}^{bin} = J_i^{bin,interface} + J_i^+ + J_i^- \qquad (56)$$

By definition, J_i^+ and J_i^- are equal to:

$$J_i^+ = \sum_{layer}^{N_{layer}-1} max(J_{tot,i}^{bin,layer}, 0) \qquad (57)$$

23

$$J_i^- = \sum_{layer}^{N_{layer}-1} min(J_{tot,i}^{bin,layer}, 0) \tag{58}$$

with $J_{tot,i}^{bin,layer}$ the total flux of condensation/evaporation/diffusion of a compound i inside a bin and a layer.

If the compound i condenses into the particle ($J_{tot,i}^{bin} > 0$), we also have $J_{cond/evap,i}^{bin} > 0$ for Eqs. (51). In that case, if the diffusion flux $J_{diff,i}^{bin,layer}$ is negative, then the compound moves by diffusion oppositely to condensation and therefore it should not be affected by the kinetic of condensation/evaporation. More generally, compounds and layers for which diffusion acts in a different direction as condensation/evaporation (fluxes of different signs) should not be affected by the kinetic of condensation/evaporation (because the compounds are transferred from one phase to another without exchange with the gas phase). In other words,

$$\text{if } J_{cond/evap,i}^{bin} \times J_{diff,i}^{bin,layer} < 0 \text{ then } J_{tot,i}^{bin,layer} = J_{diff,i}^{bin,layer} \tag{59}$$

The layers with $J_{cond/evap,i}^{bin} \times J_{diff,i}^{bin,layer} < 0$ are the layers with a diffusion flux sign opposite to $J_{tot,i}^{bin}$. Therefore, the sum over these layers allows us to compute J_i^- by Eq. (58) if $J_{tot,i}^{bin} > 0$ and J_i^+ by Eq. (57) if $J_{tot,i}^{bin} < 0$. If $J_{tot,i}^{bin} > 0$ (resp. $J_{tot,i}^{bin} < 0$), then J_i^+ (resp. J_i^-) corresponds to the part of the total flux that is affected by both condensation/evaporation and diffusion and J_i^- (resp. J_i^+) corresponds to the part of the total flux that is only affected by diffusion. J_i^- is computed by Eqs. (59) and (58) (resp. J_i^+ is computed by Eqs. (59) and (57)), and J_i^+ is deduced by Eq. (56). The total positive (resp. negative) flux J_i^+ (resp. J_i^-) is redistributed onto layers by using the weighting factors $f_i^{bin,layer}$:

$$J_{tot,i}^{bin,layer} = \frac{f_i^{bin,layer}}{\sum_{layer} f_i^{bin,layer} - f_i^{bin,interface}} J^+ \text{ (if } J_{tot,i}^{bin,layer} > 0) \tag{60}$$

$$J_{tot,i}^{bin,layer} = \frac{f_i^{bin,layer}}{\sum_{layer} f_i^{bin,layer} - f_i^{bin,interface}} J^- \text{ (if } J_{tot,i}^{bin,layer} < 0) \tag{61}$$

24

2.3.4 Characteristic time to reach equilibrium with the gas phase

The system of differential equations (48) to solve is stiff, as in the same layer/bin, some species reach equilibrium with the gas phase much quicker than others (Capaldo et al., 2000). To solve it efficiently, it is necessary to solve separately cases at equilibrium from other cases, which are solved dynamically. To determine the characteristic time to reach equilibrium with the gas phase, Eq. (48) is rewritten using the total concentrations and defining $F_i^{bin,layer} = A_{p,i}^{bin,layer}/A_{p,i}$ (if $A_{p,i}^{bin,layer}$ is different from zero):

$$\frac{dA_{p,i}^{bin,layer}}{dt} = k\left(A_{tot,i} K_{p,i}^{bin,layer} M_o^{bin,layer} - A_{p,i}^{bin,layer}\left(1 + \frac{K_{p,i}^{bin,layer} M_o^{bin,layer}}{F_i^{bin,layer}} \right) \right) \quad (62)$$

This differential equation is solved by assuming that $F_i^{bin,layer}$ and $K_{p,i}^{bin,layer} M_o^{bin,layer}$ are constant (or do not vary much over one time step):

$$A_{p,i}^{bin,layer}(t) = A_{eq} + \left(A_{p,i}^{bin,layer}(t=0) - A_{eq} \right) * exp\left(-\frac{t}{\tau_{eq}} \right) \quad (63)$$

with A_{eq} the concentration at equilibrium with the gas phase and τ_{eq} the characteristic time to reach equilibrium.

$$A_{eq} = \frac{A_{tot,i} K_{p,i}^{bin,layer} M_o^{bin,layer}}{1 + \frac{K_{p,i}^{bin,layer} M_o^{bin,layer}}{F_i^{bin,layer}}} \quad (64)$$

$$\tau_{eq}^{-1} = \left(1 + \frac{K_{p,i}^{bin,layer} M_o^{bin,layer}}{F_i^{bin,layer}} \right) k. \quad (65)$$

τ_{eq} is used to estimate the time necessary to reach equilibrium with the gas phase and therefore to identify cases that should be assumed at equilibrium when solving the system of Eq. (48)

2.3.5 Generalization to several organic phases

The organic matter can be separated into several organic phases. Whereas the evolution of condensation/evaporation is dynamically modeled, phase separation and the repartition of compounds between organic phases are assumed to be at equilibrium. They are assumed to occur
5 instantaneously: if an organic phase is saturated, it is divided instantaneously into several organic phases. The dynamic evolution due to condensation/evaporation in viscous particles is described by the following equation derived from Eq.(48) by taking into account the phase of the components:

$$
\frac{dA_{p,i}^{bin,layer,phase}}{dt} = J_{tot,i}^{bin,layer,phase} = \frac{K_{p,i}^{bin,layer,phase} M_o^{bin,layer,phase}}{\sum_{\phi}^{N_{phase}} K_{p,i}^{bin,layer,\phi} M_o^{bin,layer,\phi}} J_{tot,i}^{bin,layer} \tag{66}
$$

10 where $J_{tot,i}^{bin,layer,phase}$ is the flux of condensation/evaporation/diffusion into an organic phase. $J_{tot,i}^{bin,layer}$ is computed with the system of equations 40 to 61 generalized to several organic phases. Equation 40 is generalized into:

$$
\begin{aligned}
\frac{J_{diff}^{bin,layer}}{dt} &= \sum_{phase}^{N_{phase}} \frac{J_{diff}^{bin,layer,phase}}{dt} \\
&= \sum_{phase}^{N_{phase}} f_{morph}^{layer} k_{diffusion} (A_{g,i} K_{p,i}^{bin,layer,iphase} M_o^{bin,layer,iphase} - A_{p,i}^{bin,layer,iphase})
\end{aligned} \tag{67}
$$

with $M_o^{bin,layer,phase}$ the total organic concentrations in the specified organic phase in a spec-
15 ified bin and layer (in $\mu g\ m^{-3}$), $J_{diff}^{bin,layer,phase}$, $A_{p,i}^{bin,layer,phase}$ and $K_{p,i}^{bin,layer,phase}$ the flux of condensation/evaporation/diffusion, concentration and partitioning coefficient of the compound i for a bin, a layer and a phase.

The flux at the interface is computed via Eq. 44 using the gas-phase concentration at equilibrium with the interface:

$$A_{g,i}^{eq,bin,interface} = K_{effect} \frac{\sum_{phase}^{N_{phase}} A_{p,i}^{bin,interface,phase}}{\sum_{phase}^{N_{phase}} K_{p,i}^{bin,interface,phase} M_o^{bin,interface,phase}} \tag{68}$$

The flux of condensation/evaporation over the whole particle is computed via Eq. 51 by using the gas-phase concentration at equilibrium with a layer:

$$A_{g,i}^{eq,bin,layer} = \frac{\sum_{phase}^{N_{phase}} A_{p,i}^{bin,layer,phase}}{\sum_{phase}^{N_{phase}} K_{p,i}^{bin,layer,phase} M_o^{bin,layer,phase}} \tag{69}$$

At each time step, thermodynamic evolution is first computed. The number of organic phases and the distribution of compounds between organic phases are then computed for each layer and each bin by assuming equilibrium between phases. To compute the concentrations with several organic phases at equilibrium we first study the conditions that have to be respected. The first condition is that the activities of each compound i are equal in each phase. For example, for two phases phase$_1$ and phase$_2$:

$$\gamma_i^{bin,layer,phase_1} x_i^{bin,layer,phase_1} = \gamma_i^{bin,layer,phase_2} x_i^{bin,layer,phase_2} \tag{70}$$

The second condition, which is that each phase may be at equilibrium with the gas-phase (if condensation is too quick to be solved dynamically), can be written as:

$$\frac{A_{p,i}^{bin,layer,phase1}}{A_{p,i}^{bin,layer,phase2}} = \frac{A_{p,i}^{bin,layer,phase1}}{A_g} \times \frac{A_g}{A_{p,i}^{bin,layer,phase2}} = \frac{K_{p,i}^{bin,layer,phase1} M_o^{bin,layer,phase1}}{K_{p,i}^{bin,layer,phase2} M_o^{bin,layer,phase2}} \tag{71}$$

To respect these two conditions, the Kelvin effect must be the same for each phase.

$$\left(exp\left(-\frac{2\sigma M_{surf}^{bin}}{RT \rho_{organic} R_p} \right) \right)^{phase_1} = \left(exp\left(-\frac{2\sigma M_{surf}^{bin}}{RT \rho_{organic} R_p} \right) \right)^{phase_2} \tag{72}$$

27

M^{bin}_{surf}, $\rho_{organic}$ and σ must be the same in the two phases.

Therefore, if there are several organic phases, the partitioning coefficient must be computed with the following equation:

$$K^{bin,layer,phase}_{p,i} = \frac{760 \times 8.202 \times 10^{-5} \times T}{M^{bin,layer,phase}_{ow} \gamma^{bin,layer,phase}_{i,org} P^0_i \times 10^6} exp \left(- \frac{2\sigma M^{bin}_{surf}}{RT\rho_{organic}R_p} \right) \quad (73)$$

with M^{bin}_{surf} the mean molar mass of all organic phases at the surface of particles.

$$M^{bin}_{surf} = \frac{\displaystyle\sum_i \sum_{phase} A^{bin,surface,phase}_{p,i}}{\displaystyle\sum_i \sum_{phase} \frac{A^{bin,surface,phase}_{p,i}}{M_i}} \quad (74)$$

The characteristic times are assumed to be the same for all the organic phases to prevent a compound from being absorbed dynamically into an organic phase whereas it is at equilibrium with another organic phase. The characteristic time is then computed according to the following equation derived from Eq. (65).

$$\tau^{bin,layer,phase}_{eq} = \frac{\dfrac{1}{f^{layer}_{morph}k_{diffusion}} + \dfrac{\displaystyle\sum_{phase} K^{bin,layer,layer}_{p,i} M^{bin,layer,layer}_o}{k_{absorption}V_{layer}}}{1 + \dfrac{\displaystyle\sum_{phase} K^{bin,layer,phase}_{p,i} M^{bin,layer,phase}_o}{f^{bin,layer}_i}} \quad (75)$$

2.3.6 Absorption into the aqueous phase

For concentrations in the organic phases, the dynamic evolution follows Eq. (66) but the dynamic evolution of concentrations in the aqueous phase follows Eq. (76) because condensa-

tion/evaporation is assumed to not be limited by diffusion in the aqueous phase and a multi-layer representation is then not useful.

$$\frac{dA_{aq,i}^{bin}}{dt} = k_{absorption}\left(A_{g,i} - \frac{A_{aq,i}^{bin}}{K_{aq,i}^{bin}AQ^{bin}}\right) \tag{76}$$

2.3.7 Absorption into a particle with an aqueous phase and organic phases

5 Under most atmospheric conditions, particles are probably not entirely organic or entirely aqueous. The surface of particles is probably covered partially by both the organic matter and by the aqueous phase. Eq. (76) and (66) are still valid but $k_{absorption}$ in Eq. 76 and Eq. 45 must be corrected to take into account that there is a chance that a compound trying to condense into a phase encounters the wrong phase, i.e. a phase into which it may not condense.

10 The chance for a compound to encounter an aqueous phase $fsurf_{aq}$ is computed with Eq. 77:

$$fsurf_{aq} = \frac{S_{aq}}{S_{tot}} \tag{77}$$

with S_{aq} the surface of particles that is aqueous and S_{tot} the total surface of particles.
To evaluate this parameter, we assume that the surface of the particle is only covered by the aqueous phase and the organic phases and that the ratio of the aqueous surface over the organic
15 surface is equal to the ratio of the volume of the aqueous phase over the volume of the organic phases:

$$fsurf_{aq} = \frac{V_{aq}}{V_{aq}+V_{org}} = \frac{\frac{AQ^{bin}}{\rho_{aqueous}}}{\frac{AQ^{bin}}{\rho_{aqueous}}+\sum_{layer}^{Nlayer}\sum_{phase}^{Nphase}\frac{M_o^{bin,layer,phase}}{\rho_{organic}}} \tag{78}$$

For the condensation in the aqueous phase, by taking into account the chance for a compound to encounter the aqueous phase, $k_{absorption}$ is:

20 $$k_{absorption} = fsurf_{aq} \times 2\pi D_p D_{air} N^{bin} f(Kn,\alpha) \tag{79}$$

For the condensation in the organic phases, by taking into account the chance for a compound to encounter the organic phases, $k_{absorption}$ is:

$$k_{absorption} = (1.0 - fsurf_{aq}) \times 2\pi D_p D_{air} N^{bin} f(Kn, \alpha) \tag{80}$$

2.3.8 Redistribution of compounds between layers

To use the approach described in this paper, the mass fraction (ratio of the mass of the layer over the mass of the particle) of layers must stay constant throughout the simulation and the mass of each layer must respect the condition given by Eq. (37), which specifies the mass of the layer with respect to the total mass of the particle. However, due to rapid condensation or evaporation of the layer near the interface, concentrations of organic compounds may need to be redistributed over layers to respect this condition. If compounds are not redistributed some layers may become larger (due to the differences in fluxes) and the layer near the interface may for example become larger than the layer at the center of the particle. Moreover, as the volume of the particle changes with condensation/evaporation, the concentration of a layer can be transferred to other layers. If a particle grows due to condensation into the layer at the interface, compounds that were previously in the interface layer are "pushed" into more internal layers and the newly condensed compounds remain at the interface layer. On the opposite, if a particle shrinks due to evaporation of the layer at the interface, the missing mass of the layer will be taken from more internal layers. For a case of evaporation, the mass of the layer at the interface may be too low (due to the more rapid evolution at the interface) and the missing mass of the layer is taken from layers at the inside of the particle, i.e. concentrations are redistributed from the outside to the inside. For a case of condensation, the mass of the layer at the interface may be too high, the exceeding mass of the layer is redistributed over the layers at the inside of the particle, i.e. concentrations are redistributed from the inside to the outside. The algorithm is detailed in Table 3.

The redistribution algorithm creates numerical diffusion as a small fraction of the mass of a layer is always transferred to other layers. This redistribution effect should decrease if the number of layers increases but it is necessary for 3D application to keep the number of layers

low. However, the redistributed amount should be low compared to absorbed amount of organic compounds. Similarly, in 3D air quality model, concentrations and number of particle in size sections have to be redistributed between sections so that the bounds diameters of sections are kept constant, which does also create some numerical issues. In SOAP, the diameters of sec-
5 tions evolve according to the mass that condenses or evaporates (without changing the number in sections) and there is no size redistribution between sections. However, a size-section redistribution algorithm should be added to the code if coagulation is added (for modeling purposes) or in 3D models (in which SOAP would be implemented) after the call of SOAP.

2.3.9 Thermodynamic equilibrium

10 For numerical stability, some compounds in some bins and layers are assumed to be at equilibrium with the gas phase because equilibrium is reached very fast (for example for very volatile compounds). To identify cases where equilibrium with the gas phase should be assumed, a criterion $t_{equilibrium}$ is used. If the characteristic time to reach equilibrium with the gas phase is lower than $t_{equilibrium}$, the case is considered at equilibrium whereas if it is higher than
15 $t_{equilibrium}$, the case is solved dynamically.

Concentrations of organic compounds in the organic phases are computed according to Eq. (81) (obtained by generalizing Eq. 2 for several bins, layers and phases):

$$A_{p,i}^{bin,layer,phase} = conc_{i,eq} \frac{K_{p,i}^{bin,layer,phase} M_o^{bin,layer,phase}}{1 + ratio_{i,eq}} \tag{81}$$

with $conc_{i,eq}$ the total concentration of compound i at equilibrium with the gas phase (sum of the
20 gas-phase concentration and of organic-phase concentrations in layers and bins at equilibrium) computed with Eq. (82) and $ratio_{i,eq}$ the ratio of the concentration of compound i at equilibrium with the gas phase in the particle phase to the concentration of i in the gas phase computed with Eq. (83) (similar to Eq. (15) for several bins, layers and phases).

$$conc_{i,eq} = A_{tot,i} - \sum_{bin} \sum_{layer} \sum_{phase} (1 - \lambda^{bin,layer,phase}) A_{p,i}^{bin,layer,phase} \tag{82}$$

31

$$
\begin{aligned}
ratio_{i,eq} &= \frac{\displaystyle\sum_{bin}\sum_{layer}\sum_{phase} \lambda^{bin,layer,phase} A_{p,i}^{bin,layer,phase}}{A_g} \\
&= \sum_{bin}\sum_{layer}\sum_{phase} \lambda^{bin,layer,phase} K_{p,i}^{bin,layer,phase} M_o^{bin,layer,phase}
\end{aligned}
\tag{83}
$$

With $\lambda^{bin,layer,phase}$ defined such as:

$$
\begin{aligned}
\lambda^{bin,layer,phase} &= 1 \quad \text{if } \tau_{eq}^{bin,layer,phase} < t_{equilibrium} \text{ (case at equilibrium)} \\
&= 0 \quad \text{if } \tau_{eq}^{bin,layer,phase} >= t_{equilibrium} \text{ (dynamic case)}
\end{aligned}
\tag{84}
$$

5   The system is solved iteratively, as now detailed. The composition of the particles is first estimated using Eq. (81) to (84). If the concentrations computed from this estimation are different from those obtained in the previous iteration, a new estimation of concentrations is computed. The algorithm is detailed in Table 1. Step 7 and step 2 prevent the non-convergence due to high variations of concentrations by reducing the variations between two iterations.

10 Some numerical issues can arise from the equilibrium representation especially for low volatility compounds with high value of $t_{equilibrium}$ (for example 100 s). For these compounds, assuming equilibrium with the gas phase will give errors because these compounds will condense almost entirely on the bin with the higher organic mass instead of condensing on each bin according to the kinetics of condensation. To prevent this problem, low volatility cases (with
15 $K_{p,i}^{bin,layer,phase} > 10$) are assumed dynamic.

2.3.10 Methodology used to compute the evolution of concentrations

The method used to solve the evolution of concentrations is shown in Fig. 5. As mentioned in the previous section, the model uses a hybrid method combining a dynamic representation where concentrations evolve as a function of time (for cases with characteristic times higher
20 than a $t_{equilibrium}$ value specified by the user) with an equilibrium representation (for cases with characteristic times lower than the $t_{equilibrium}$ value). In the equilibrium representation,

32

the distribution of organic compounds between phases and the gas/particle partitioning of cases with characteristic times lower than $t_{equilibrium}$ are computed.

In the dynamic representation, concentrations evolving dynamically (cases with characteristic times higher than $t_{equilibrium}$) are computed as a function of the time step with the second-order Rosenbrock scheme ROS2 (Verwer et al., 1999) for time integration. The time step can be rejected (the computation is redone with another time step) if the error between the second order and the first order concentrations is too high (higher than an EPSER parameter specified by the user). In that case, the time step decreases until the error is lower than EPSER (until the time step is accepted). If the time step is very low, the ROS2 scheme increases the time step to obtain the optimal time step.

To compute concentrations, the model first initializes required properties (activity coefficients, the number of phases in each layer and the characteristic times). For the first time step, the model calls a first time the equilibrium representation. Once the equilibrium is reached, the model computes the dynamic evolution with the dynamic representation. Because concentrations changed, the gas/particle partitioning of cases at equilibrium changed, the equilibrium representation is then called again. For the next time steps, the dynamic and equilibrium representations are called once each, until the ending time of the simulation is reached.

3 Results

In this section, the dynamic implicit representation of SOAP is first compared to an explicit representation to check that the dynamic evolution of surrogates between the gas and particle phases is well represented by the implicit representation. Two test cases representative of European summer periods with high biogenic concentrations and high anthropogenic concentrations are then defined. Simulations are performed to study the impact of ideality, saturation, phase separation and thermodynamic equilibrium on the model results. Comparisons of the implicit and explicit representations for one of the test case are also performed.

33

3.1 Validation of the dynamic implicit representation

To validate the dynamic implicit representation of SOAP, we study the condensation of an hydrophobic organic surrogate of different volatilities (with a partitioning coefficient of 100, 1, or 0.01 m^3/μg) for different organic-phase diffusion coefficients (10^{-19} m^2/s, 10^{-20} m^2/s, 10^{-21} m^2/s, 10^{-22} m^2/s and 10^{-24} m^2/s) into 5 μg m^{-3} of non-volatile organic compounds. The organic surrogate that condenses is initially only in the gas phase, with a mass of 5 μg m^{-3}. The size distribution of particles is divided into 5 bins. The number of particles inside bin is taken equal to 3.02×10^8, 1.40×10^9, 2.24×10^8, 1.69×10^6, 12224.0 particles/m^3 based on average simulation results over Europe (Couvidat et al., 2012a). The initial mass concentrations of the surrogate is distributed between each section with the following fraction: 0.7%, 26.6%, 61.4%, 11.2%, 0.1%. The initial diameter of each bin is computed from the initial mass and number concentrations in the bin.

The results of the implicit representation are compared with an explicit representation where diffusion between layers is treated explicitly. In the explicit representation, the diffusion of organic compounds in the particle is represented explictly as in KM-GAP (with no equilibrium assumption). The particles are discretized with 100 layers, each of them having a volume representing 1% of the total volume of the particles. The evolution of concentrations inside each layer i is computed by:

$$C_i(t + \Delta t) = C_i(t) + \frac{F_{i,i+1} + F_{i,i-1}}{V_{layer}} \Delta t \tag{85}$$

with $F_{i,i+1}$ and $F_{i,i-1}$, the fluxes of diffusion between the layer i and the nearby layers (the computation of those fluxes is given in the supplementary materials) and V_{layer} the volume of the layer. As in the implicit representation, the volume of each layer is kept constant throughout the simulation using the redistribution scheme presented in section 2.3.8.

Fig. 6 shows the comparison between the explicit representation with 100 layers and the implicit representation with 4 and 5 layers (one of this layer being the interface layer not affected by diffusion). The implicit representation reproduces well the result of the explicit representation. For non-volatile compounds (with a partitioning coefficient around 100 m^3/μg), there is no

34

significant differences between the two methods. For such compounds, the condensation is not limited by diffusion and therefore they condense independently of the organic-phase diffusion coefficient. For low volatility compounds (with a partitioning coefficient around 1 $m^3/\mu g$), first, condensation into the first layer occurs without a limitation due to diffusion and then diffusion over all the particle occurs. The implicit representation with 5 layers slightly underestimates the diffusion of low volatility compounds for low organic-phase diffusion coefficients (10^{-19} m^2/s) but reproduces very well cases with lower diffusion coefficients (lower than 10^{-20} m^2/s) whereas the implicit representation with 4 layers slightly overestimates the diffusion of low volatility compounds. For more volatile compounds (with a partitioning coefficient around 0.01 $m^3/\mu g$), the implicit representation reproduces well the explicit representation with both 4 and 5 layers but underestimates low concentrations (lower than 10% of the concentration at equilibrium) with 4 layers.

To fully validate the implicit representation, a comparison of the implicit and explicit representations is also performed for one of the test case (see section 3.5).

3.2 Set-up of the test cases

The behavior of the model is tested using two test cases. The first test case corresponds to a summer period with high concentrations of biogenic SOA, and the second test case corresponds to a summer period with high concentrations of anthropogenic SOA. These two test cases are referred hereafter as the "biogenic test case" and the "anthropogenic test case". For the biogenic and the anthropogenic test cases, pollutant mass concentrations and meteorological conditions are extracted from the simulations of Couvidat et al. (2012a) and Couvidat et al. (2012b) over Europe and Paris area respectively.

The surrogates are the same as in the aerosol model H^2O, which was used by Couvidat et al. (2012a,b). Surrogates are described in Table 4 and their total concentrations (gas + particle) are given in Table 5 for both test cases. For both test cases, the liquid water content of aerosol, the pH, the ionic strength and the concentrations of inorganic ions are computed with the ISOR-ROPIA model (Nenes et al., 1998) at a specified relative humidity (RH). In H^2O, the surrogates that are representative of primary and aged SVOC (POAlP, POAmP, POAhP, SOAlP, SOAmP

35

and SOAhP) do not have a molecular structure attached. Therefore processes depending on the molecular structure (like absorption on the aqueous phase) are not estimated for those surrogates. They are assumed to be hydrophobic and their influence on the activity coefficients of other species is taken into account by assigning to them a default molecular structure representative of primary aerosol and lowly oxidized compounds. This default structure is constituted of 40% of $C_{23}H_{47}COOH$, 5% of $C_8H_{17}CH=CHC_7H_{14}COOH$, 15% of 4-(2-propio)-syringone, 12% of $C_{29}H_{60}$ and 28% of 2-carboxybenzoic acid based on (EPRI, 1999). In our test cases, the same default structure as in H^2O is used.

The size distribution and the number of particles are the same as those used for the validation. The volume of the solid core of each size section is computed from the mass concentrations of solid species (dust, black carbon, solid inorganic given by ISORROPIA) to compute morphology factors.

3.3 Equilibrium representation

To study the impact of activity coefficients, hydrophilic properties of surrogates, saturation and phase separation, concentrations in the particle phase are assumed to be at equilibrium with the gas phase for all surrogates.

3.3.1 Influence of activity coefficients on organic aerosol formation (without phase separation of the organic phase)

The effect of non-ideality on aerosol concentrations is strong and complex. To determine the impact of non-ideality, tables 6 and 7 show the concentrations of organic aerosol for both test cases formed from the various precursors as well as the concentrations of water, with and without the ideality assumption, respectively. The compounds are assumed to be both hydrophilic and hydrophobic except for the species POAlP, POAmP, POAhP, SOAlP, SOAmP and SOAhP, which are simply assumed to be hydrophobic, with the default molecular structure used in Couvidat et al. (2012a).

Concentrations of compounds in the organic phase tend to decrease strongly when non-

ideality is assumed (except for aromatics in the biogenic case due to non-linear effects), especially for the compounds formed from isoprene oxidation (most of them are very hydrophilic and therefore have low affinity with very hydrophobic compounds) and for some of the compounds formed from monoterpenes. Concentrations of hydrophilic compounds in the aqueous
5 phase either increase or decrease depending on conditions. For the compounds formed from isoprene oxidation, their concentrations increase in the biogenic case from 0.70 μg m^{-3} for ideality to 1.24 μg m^{-3} for non-ideality with long, medium and short ranges interactions and to 1.29 μg m^{-3} for non-ideality with only short-range interactions. It seems to indicate that in this case short-range interactions between organic compounds tend to stabilize hydrophilic organic
10 compounds in the aqueous phase whereas medium-range and long-range interactions between organic and inorganic compounds tend to destabilize hydrophilic organic compounds. These results are consistent with the result of Couvidat et al. (2012a) where assuming ideality at infinite dilution can lead to an underestimation of the concentrations of hydrophilic species inside the aqueous phase of particles. Therefore, the concentrations of hydrophilic organic compounds
15 in the aqueous phase probably depend strongly on other compounds and on the non-ideality of aerosols.

3.4 Hydrophobic versus hydrophilic

Determining a priori if a compound is hydrophilic or hydrophobic is not straightforward. Ta-
20 ble 8 shows that some compounds seem clearly hydrophobic (BiA2D, BiA1D, AnBlP, BiBlP, BiBmP, AnClP, BiNGA, BiNIT3, BiNIT) or hydrophilic (BiA0D) as they partition only into one phase. However, some compounds are present in both the organic and aqueous phases. AnBmP seems to be both hydrophilic and hydrophobic and can change phase depending on conditions. Moreover, BiA2D, BiA1D and BiMGA were assumed to be hydrophilic in H^{2}O
25 whereas it seems from these test cases that they are mainly hydrophobic. The fact that these compounds were assumed hydrophilic is probably due the choice of a criterion not representative of all atmospheric conditions. BiA2D and BiA1D were assumed hydrophilic based on their octanol/water coefficient (Pun et al., 2006), which is probably not representative of atmospheric

37

conditions. BiMGA was assumed hydrophilic based on the results of Couvidat and Seigneur (2011). According to this study, BiMGA condenses mostly on the aqueous phase if the liquid water content of aerosols is high (superior to the concentration of the organic phase), which is not the case in the two test cases. Moreover, if medium-range and long-range interactions

5   are not taken into account, the distribution of the compounds between phases change significantly. For the biogenic test case, if medium-range and long-range interactions are not taken into account as in Couvidat and Seigneur (2011), the fraction in the organic phase decreases from 75% to 33% for particulate BiA2D and from 89% to 46% for particulate BiA1D. For the anthropogenic test case, the fraction in the organic decreases, from 99% to 76% for particu-

10 late BiA2D, from 100% to 85% for particulate BiA1D and from 59% to 46% for particulate BiMGA. It is therefore possible for these compounds to be present in both phases depending on conditions.

3.4.1   Saturation and phase separation

Species having very different properties do not mix well together and phase separation can

15 be computed by Gibbs energy minimization (see section 2.2.4). Table 9 presents the concentrations with or without phase separation for the biogenic test case at RH=30% without an aqueous phase. In this case, without phase separation, both hydrophilic and hydrophobic compounds want to condense into the organic phase which is mainly constituted by hydrophobic compounds. Assuming phase separation in this case does not strongly influence concentrations

20 of hydrophobic compounds, which decrease slightly. However, a second organic phase is created by phase separation which is constituted mainly by very oxidized compounds (BiPER, BiDER and BiMGA). For the anthropogenic case, at RH=30%, phase separation do not happen because the concentrations of hydrophilic compounds are too low for the organic phase to be saturated.

25 Another organic phase may be created if there are compounds with low oxidation state. For the biogenic case at low humidity, if the structure of nonadecane is used to represent the compounds POAlP, POAmP, POAhP, SOAlP, SOAmP and SOAhP (without a molecular structure; these compounds only condense into the less oxidized phase without impacting phase sepa-

38

ration), a third organic phase may be created. Compounds with low oxidation state may not readily mix with slightly oxidized compounds which in turn may not readily mix with more oxidized compounds.

3.5 Dynamic representation

For the dynamic modelling, users must choose the organic-phase diffusion coefficients because there is currently, to our knowledge, no method to estimate diffusion coefficients of the organic phase as a function of the composition of organic aerosols. In this section, the same organic-phase diffusion coefficient is used for all organic compounds. For all the compounds, the gas-phase diffusion coefficient is taken equal to 0.1 cm^2/s which is the order of magnitude of this parameter (Seinfeld and Pandis, 1998) and the accommodation coefficient (value between 0 and 1) is taken equal to 0.01 so that it corresponds to the order of magnitude of accommodation coefficients for organic compounds given in other studies (between 0.1 (Saleh et al., 2013) and 0.001 (Lee et al., 2011)). The gas-phase diffusion coefficient and the accommodation coefficient are used in Eq. (79) and (80).

In the regional-scale simulations from which initial concentrations are extracted, equilibrium is assumed between gas and particles. For the dynamic modelling, 5 μg m^{-3} of non-volatile hydrophobic organic compounds is added to have a mass into which compounds are not present and will have to diffuse. For each surrogate, the total mass gas + particles is kept the same as in the equilibrium simulations. However, the particle-phase concentrations are taken equal to 10% of the equilibrium particle-phase concentrations.

To fully validate the implicit representation of the dynamic evolution of surrogates, the results of SOAP are compared to the results of the explicit representation for the biogenic test case assuming ideality. RH is assumed to be equal to 30%. Results of this comparison are shown in Fig. 7. This results shows good results with 5 layers and a slight overestimation with 4 layers of OM concentrations due to the overestimation of condensation for low volatility compounds.

The dynamic implicit representation is tested for various humidities and various diffusion coefficients for the biogenic and anthropogenic cases. Figures 8 and 9 show the concentrations in the organic phases for the biogenic and anthropogenic cases respectively whereas Figures

39

10 and 11 show concentrations in the aqueous phase for the biogenic and anthropogenic cases respectively. The influence of the number of layers is also tested in these figures.

The two test cases show similar results. For the condensation into the organic phases, the growth of particles can be divided into two parts. The particle grows by condensation into the layer at the interface independently from the viscosity of the organic phases until the growth of particle become limited by the diffusion of the more volatile compounds into the organic phases. For the anthropogenic test case, humidity has a low effect between 30% to 70% on the condensation of organic compounds into the organic phases because they are mainly constituted of hydrophobic compounds in the anthropogenic test case. However, at 70% more hydrophilic compounds manage to condense into the aqueous phase. Between 70% to 90%, the amount of organic compounds in the organic phases decreases whereas the amount of organic compounds increases in the aqueous phase. For the biogenic test case, the organic phase concentration increases between 30% and 50% of humidity because hydrophilic compounds (which are in higher concentrations than in the anthropogenic test case) partition more efficiently. Between 30% and 70%, the organic-phase concentration decreases but the aqueous-phase concentration increases because hydrophilic compounds condense more efficiently into the aqueous phase. However, diffusion coefficients are probably much higher at high humidity than at low humidity because the organic phases would be less viscous (less oligomerization due to esterification for example and more water in the organic phases which would decrease viscosity) as shown by Saukko et al. (2012); Renbaum-Wolff et al. (2013). It may then be possible that at high humidity, organic aerosols reach equilibrium quicker than at low humidity. A method to estimate diffusion coefficients as a function of composition (or at least of as a function of humidity) is needed to properly represent this phenomenon.

3.6 Time analysis

Table 10 shows the computation time necessary to solve the biogenic case at RH=70% (relative to the time necessary to solve the case with an uncoupled and ideal system) for different configurations of the model. For the dynamic approach, 4 layers are used, the length of the computation corresponds to 600s (corresponding to a time step of a simulation with the Polyphemus air qual-

40

ity platform over Europe (Sartelet et al., 2007)), initial concentrations are assumed to be 80% of concentrations at equilibrium and an organic phase diffusion coefficient of 10^{-21} m²/s is used. The times given here correspond to a specific case and therefore can greatly vary with initial conditions and with the chosen parameters for the numerical resolution of the system. They are
5 provided here on an indicative basis. The dynamic approach is around 400 times slower than the equilibrium approach, making its applicability limited to short-term 3D simulations.

More reliable and complete information about the computation time cost will be provided in future studies about the implementation of the SOAP in an air quality model.

4 Conclusions

10 The Secondary Organic Aerosol Processor model is a modular model, which can compute the condensation/evaporation of organic aerosol according to two different approaches: an equilibrium approach and a dynamic approach. In the equilibrium approach, concentrations in the particle phase are assumed at equilibrium with concentrations in the gas phase. In the dynamic approach, concentrations evolve according to the kinetics of condensation/evaporation/diffusion
15 of organic compounds. The dynamic approach uses a multi-layer representation of particles to represent the particle-phase diffusion of organic compounds. Future works will focus on improving the framework of this dynamic approach to take into account varying diffusion coefficients with layers, to allow entrapment of compounds in inner layers and to represent layer exchanges and transfers between the organic and the aqueous phases. Simulations with SOAP
20 and comparisons to measurements should be performed to validate the model and to test the influence of each process and parameter on organic aerosol formation.

To improve the representation of aerosols, several processes should be added to the model. First, interactions between organic and inorganic compounds should be fully taken into account via activity coefficients. Currently, only the influence of inorganic compounds on organic
25 compounds is taken into account. However, organic compounds can also impact the formation of inorganic compounds due to those interactions. This process could be taken into account by adding inorganic aerosol formation to SOAP. Second, a method to estimate diffusion

41

coefficients in organic phases should be developed, as it is expected that composition of the organic phases greatly influences the viscosity and therefore diffusion coefficients of organic compounds. Finally, the model could be coupled to a solver for particle-phase chemistry and then represent processes such as oligomerization, which could affect the viscosity of the organic phases.

5 Notations

A_{eq}	the concentration in the organic phase at equilibrium
$A_{g,i}$	the concentration of i in the gas phase (in $\mu g\,m^{-3}$)
$A_{g,i}^{eq,bin}$	the concentration of i in the gas phase (in $\mu g\,m^{-3}$) at equilibrium with the whole particle
$A_{g,i}^{eq,bin,interface}$	the concentration of i in the gas phase (in $\mu g\,m^{-3}$) at equilibrium with the interface layer
$A_{g,i}^{eq,bin,layer}$	the concentration of i in the gas phase (in $\mu g\,m^{-3}$) at equilibrium with the layer
$A_{p,i}$	the concentration of i in the organic phase (in $\mu g\,m^{-3}$)
$A_{p,i}^{phase}$	the concentration of i in the organic phase (in $\mu g\,m^{-3}$) in a phase
$A_{p,i}^{bin}$	the concentration of i in the organic phase (in $\mu g\,m^{-3}$) in a diameter bin
$A_{p,i}^{bin,layer}$	the concentration of i in the organic phase (in $\mu g\,m^{-3}$) in a diameter bin/layer
$A_{p,i}^{bin,layer,phase}$	the concentration of i in the organic phase (in $\mu g\,m^{-3}$) in a bin/layer/phase
$A_{p,i}^{bin,interface}$	the concentration of i in the organic phase (in $\mu g\,m^{-3}$) in a diameter bin at the interface layer

$A_{p,i}^{bin,interface,phase}$	the concentration of i in the organic phase (in μg m^{-3}) in a bin/phase at the interface layer
$A_{p,water}$	the concentration of water in the organic phase (in μg m^{-3})
$A_{aq,i}$	the concentration of i in the aqueous phase (in μg m^{-3})
$A_{aq,i}^{bin}$	the concentration of i in the aqueous phase in a diameter bin (in μg m^{-3})
$A_{tot,i}$	the concentration of i in all phases (in μg m^{-3})
AQ	total mass of the aqueous phase including organic compounds (in μg m^{-3})
AQ_{inorg}	total mass of the aqueous phase excluding organic compounds (in μg m^{-3})
AQ^{bin}	total mass of the aqueous phase including organic compounds in a bin (in μg m^{-3})
C	concentration (in M)
C_s	concentration at the surface of the particle (in M)
D_p	diameter of the particle (in m)
D_{air}	diffusivity of the compound in air (in m^2/s)
D_{org}	diffusivity of the compound in the organic phase (in m^2/s)
$F_i^{bin,layer}$	fraction of $A_{p,i}$ in a diameter bin/layer
$f_i^{bin,layer}$	factor of weighting according to the diffusion fluxes
f_{morph}^{layer}	morphology factor
$fsurf_{aq}$	the chance for a compound to encounter an aqueous phase at the surface of the particle
f(Kn,α)	transition regime formula
f_s	volume of the solid phase in the particle over the volume of the particle
G	Gibbs energy
H_i	Henry's law constant (in M/atm)

$J^{bin}_{cond/evap,i}$	Flux of condensation/evaporation (in μg m^{-3} s^{-1}) inside the whole particle
$J^{bin}_{diff,i}$	Flux of diffusion (in μg m^{-3} s^{-1}) inside the whole particle
$J^{bin,layer}_{diff,i}$	Flux of diffusion (in μg m^{-3} s^{-1}) inside a bin/layer
$J^{bin,layer,phase}_{diff,i}$	Flux of diffusion (in μg m^{-3} s^{-1}) inside a bin/layer/phase
$J^{bin,interface}_{i}$	Flux of condensation/evaporation (in μg m^{-3} s^{-1}) at the interface layer
$J^{bin}_{tot,i}$	Flux of condensation/evaporation/diffusion (in μg m^{-3} s^{-1}) inside the whole particle
$J^{bin,layer}_{tot,i}$	Flux of condensation/evaporation/diffusion (in μg m^{-3} s^{-1}) inside a bin/layer
$J^{bin,layer,phase}_{tot,i}$	Flux of condensation/evaporation/diffusion (in μg m^{-3} s^{-1}) inside a bin/layer/phase
J^{+}_{i}	sum of the positive diffusion fluxes $J^{bin,layer}_{diff,i}$
J^{-}_{i}	sum of the negative diffusion fluxes $J^{bin,layer}_{diff,i}$
$K_{aq,i}$	the aqueous-phase partitioning coefficient
$K^{bin}_{aq,i}$	the aqueous-phase partitioning coefficient of a diameter bin
$K_{p,i}$	the organic-phase partitioning coefficient
$K^{phase}_{p,i}$	the organic-phase partitioning coefficient for a phase
$K^{bin,layer}_{p,i}$	the organic-phase partitioning coefficient of a diameter bin/layer
$K^{bin,layer,phase}_{p,i}$	the organic-phase partitioning coefficient of a diameter bin/layer/phase
$K^{bin,interface}_{p,i}$	the organic-phase partitioning coefficient of a diameter bin at the interface layer
$K^{bin,interface,phase}_{p,i}$	the organic-phase partitioning coefficient of a diameter bin/phase at the interface layer
k	kinetic rate parameter of the absorption-diffusion equation

$k_{absorption}$	kinetic rate parameter of the absorption equation
$k_{diffusion}$	kinetic rate parameter of the diffusion equation
K_{effect}	Kelvin effect correction
Kn	Knudsen number
N_{layer}	number of layers
N_{layer}^{dif}	number of layers into which diffusion occurs
M_{aq}	mean molar mass of the aqueous phase (in g/mol)
M_i	mean molar mass of i (in g/mol)
m_i	mass of i in a particle
m_i^{bin}	mass of i in a particle of the bin
M_o	concentration of the organic phase (in μg m^{-3})
M_o^{phase}	concentration of the organic phase (in μg m^{-3}) for a phase
M_o^{bin}	concentration of the organic phase in a diameter bin (in μg m^{-3})
$M_o^{bin,layer}$	concentration of the organic phase in a diameter bin/layer (in μg m^{-3})
$M_o^{bin,layer,phase}$	concentration of the organic phase in a diameter bin/layer/phase (in μg m^{-3})
$M_o^{bin,interface}$	concentration of the organic phase at the interface layer in a diameter bin (in μg m^{-3})
$M_o^{bin,interface,phase}$	concentration of the organic phase at the interface layer in a diameter bin/phase (in μg m^{-3})
M_{ow}	mean molar mass of the organic phase (in g/mol)
M_{water}	molar mass of water
n_i^{ϕ}	number of moles of compound i in the phase ϕ
N^{bin}	number of particles in a diameter bin (in m^{-3})
P_i^0	the saturation vapor pressure of i
P_i	partial pressure of i

$P_{eq,i}$	partial pressure of i at equilibrium (taking into account the Kelvin effect)
R	the ideal gas constant
R_p	the rayon of the particle (in m)
S_{aq}	surface of particles covered by an aqueous phase
S_{tot}	surface of particles
RH	the relative humidity
T	the temperature
T_{ref}	the temperature of reference at which P_i^0 is determined
V_{layer}	volume fraction of the layer
V_{aq}	volume of the aqueous phase
V_{org}	volume of the organic phase
$X_{i,aq}$	molar fraction of i in the aqueous phase
$X_{i,org}$	molar fraction of i in the organic phase
α	accommodation coefficient
α_{layer}	ratio of the characteristic time for diffusion of the layer to the characteristic time for diffusion of the center of the particle
$\gamma_{i,aq}$	activity coefficient of i in the aqueous phase
$\gamma_{i,aq}^{\infty}$	activity coefficient of i at infinite dilution in water
$\gamma_{i,org}$	activity coefficient of i in the organic phase
$\gamma_{water,aq}$	activity coefficient of water in the aqueous phase
$\gamma_{water,org}$	activity coefficient of water in the organic phase
ΔH_i	enthalpy of vaporization of i (in J/mol)
μ_i^{ϕ}	chemical potential of i
ξ_i	activity coefficient of i in the aqueous phase by reference to infinite dilution
τ_{dif}	characteristic time for diffusion
τ_{eq}	characteristic time to reach equilibrium

References

Abramson, E., Imre, D., Beránek, J., Wilson, J., and Zelenyuk, A.: Experimental determination of chemical diffusion with secondary organic aerosol particles, Phys. Chem. Chem. Phys., 15, 2983–2991, doi:10.1039/C2CP44013J, 2013.

Capaldo, K. P., Pilinis, C., and Pandis, S. N.: A computationally efficient hydbrid approach for dynamic gas/aerosol transfer in air quality models, Atmos. Environ., 34, 3617–3627, doi:10.1016/S1352-2310(00)00092-3, 2000.

Cappa, C. D. and Wilson, K. R.: Evolution of organic aerosol mass spectra upon heating: implications for OA phase and partitioning behavior, Atmos. Chem. Phys., 11, 1895–1911, doi:10.5194/acp-11-1895-2011, 2011.

Choi, M. Y. and Chan, C. K.: The effects of organic species on the hygroscopic behaviors of inorganic aerosols, Environ. Sci. Tech., 36, 2422–2428, doi:10.1021/es0113293, 2002.

Couvidat, F. and Seigneur, C.: Modeling secondary organic aerosol formation from isoprene oxidation under dry and humid conditions, Atmos. Chem. Phys., 11, 893–909, doi:10.5194/acp-11-893-2011, 2011.

Couvidat, F., Debry, É., Sartelet, K., and Seigneur, C.: A Hydrophilic/Hydrophobic Organic (H^{2}O) model: Model development, evaluation and sensitivity analysis, J. Geophys. Res., 117, D10 304, doi:10.1029/2011JD017214, 2012a.

Couvidat, F., Kim, Y., Sartelet, K., Seigneur, C., Marchand, N., and Sciare, J.: Modeling secondary organic aerosol in an urban area: Application to Paris, France, Submitted to Atmos. Chem. Phys., 2012b.

EPRI: Organic Aerosol Partition Module Documentation, EPRI, Palo Alto, CA, USA, *Technical Report*, 1999.

Erdakos, G. B. and Pankow, J. F.: Gas/particle partitioning of neutral and ionizing compounds to single and multi-phase aerosol particles. 2. Phase separation in liquid particulate matter containing both polar and low-polarity organic compounds, Atmos. Environ., 38, 1005–1013, doi:10.1016/j.atmosenv.2003.10.038, 2004.

Fredenslund, A., Jones, R. L., and Prausnitz, J. M.: Group-contribution estimation of activity-coefficients in nonideal liquid-mixtures, AIChE J., 21, 1086–1099, 1975.

Fuchs, N. and Sutugin, A.: Topics in current aerosol research (part 2), chap. High dispersed aerosols, Pergamon, New york, 1971.

Griffin, R. J., Nguyen, K., Dabdub, D., and Seinfeld, J. H.: A coupled hydrophobic-hydrophilic model

47

for predicting secondary organic aerosol formation, J. Atmos. Chem., 44, 171–190, doi:10.1023/A:1022436813699, 2003.

Kanakidou, M., Seinfeld, J. H., Pandis, S. N., Barnes, I., Dentener, F. J., Facchini, M. C., Van Dingenen, R., Ervens, B., Nenes, A., Nielsen, C. J., Swietlicki, E., Putaud, J. P., Balkanski, Y., Fuzzi, S., Horth, J., Moortgat, G. K., Winterhalter, R., Myhre, C. E. L., Tsigaridis, K., Vignati, E., Stephanou, E. G., and Wilson, J.: Organic aerosol and global climate modelling: a review, Atmos. Chem. Phys., 5, 1053–1123, doi:10.5194/acp-5-1053-2005, 2005.

Katrinak, K. A., Rez, P., Perkes, P. R., and Buseck, P. R.: Fractal geometry of carbonaceous agregates from an urban aerosol, Environ. Sci. Technol., 27, 539–547, doi:10.1021/es00040a013, 1993.

Larson, S. M., Cass, G. R., and Gray, A. H.: Atmospheric Carbon Particles and the Los Angeles Visibility Problem, Aerosol Sci. Technol., 10, 118–130, doi:10.1080/02786828908959227, 1989.

Lee, B.-H., Pierce, J. R., Engelhart, G. J., and Pandis, S. N.: Volatility of secondary organic aerosol from the ozonolysis of monoterpenes, Atmos. Environ., 45, 2443–2452, doi:10.1016/j.atmosenv.2011.02.004, 2011.

Nenes, A., Pandis, S. N., and Pilinis, C.: ISORROPIA: A new thermodynamic equilibrium model for multiphase multicomponent inorganic aerosols, Aquat. Geoch., 4, 123–152, 1998.

Pankow, J. F.: An absorption model of gas/particle partitioning of organic compounds in the atmosphere, Atmos. Environ., 28A, 185–188, 1994.

Pfrang, C., Shiraiwa, M., and Pöschl, U.: Chemical ageing and transformation of diffusivity in semi-solid multi-component organic aerosol particles, Atmos. Chem. Phys., 11, 7343–7354, doi:10.5194/acp-11-7343-2011, 2011.

Pun, B. K., Griffin, R. J., Seigneur, C., and Seinfeld, J. H.: Secondary organic aerosol. 2. Thermodynamic model for gas/particle partitioning of molecular constituents, J. Geophys. Res., 107, 433, doi:10.1029/2001JD000542, 2002.

Pun, B. K., Seigneur, C., and Lohman, K.: Modeling secondary organic aerosol formation via multiphase partitioning with molecular data, Environ. Sci. Technol., 40, 4722–4731, doi:10.1021/es0522736, 2006.

Renbaum-Wolff, L., Grayson, J. W., Bateman, A. P., Kuwata, M., Sellier, M., Murray, B. J., Shilling, J. E., Martin, S. T., and Bertram, A. K.: Viscosity of α-pinene secondary organic material and implications for particle growth and reactivity, Proc. Natl. Acad. Sci., doi:10.1073/pnas.1219548110, http://www.pnas.org/content/early/2013/04/24/1219548110.abstract, 2013.

Robinson, R. A. and Stokes, R. H.: Electrolyte solutions, 2nd (revised) edition; Butterworth, 1965.

Sachdeva, K. and Attri, A. K.: Morphological characterization of carbonaceous aggregates in soot

and free fall aerosol samples, Atmos. Environ., 42, 1025–1034, doi:10.1016/j.atmosenv.2007.10.002, 2007.

Saleh, E., Donahue, N. M., and Robinson, A. L.: Time Scales for Gas-Particle Partitioning Equilibration of Secondary Organic Aerosol Formed from Alpha-Pinene Ozonolysis, Environ. Sci. Technol., 47, 5588–5594, doi:10.1021/es400078d, 2013.

Sartelet, K., Debry, E., Fahey, K., Roustan, Y., Tombette, M., and Sportisse, B.: Simulation of aerosols and gas-phase species over Europe with the Polyphemus system. Part I: model-to-data comparison for 2001, Atmos. Environ., 41, 6116–6131, doi:10.1016/j.atmosenv.2007.04.024, 2007.

Saukko, E., Lambe, A. T., Massoli, P., Koop, T., Wright, J. P., Croasdale, D. R., Pedernera, D. A., Onasch, T. B., Laaksonen, A., Davidovits, P., Worsnop, D. R., and Virtanen, A.: Humidity-dependent phase state of SOA particles from biogenic and anthropogenic precursors, Atmos. Chem. Phys., 12, 7517–7529, doi:10.5194/acp-12-7517-2012, 2012.

Seinfeld, J. and Pandis, S.: Atmospheric chemistry and physics: from air pollution to climate change, Wiley-interscience, 1998.

Shiraiwa, M. and Seinfeld, J. H.: Equilibration timescale of atmospheric secondary organic aerosol partitioning, Geophys. Res. Lett., 39, L24 801, doi:10.1029/2012GL054008, 2012.

Shiraiwa, M., Ammann, M., Koop, T., and Pöschl, U.: Gas uptake and chemical aging of semisolid organic aerosol particles, Proc. Natl. Acad. Sci., 108, 11 003–11 008, doi:10.1073/pnas.1103045108, 2011.

Shiraiwa, M., Pfrang, C., Koop, T., and Pöschl, U.: Kinetic multi-layer model of gas-particle interactions in aerosols and clouds (KM-GAP): linking condensation, evaporation and chemical reactions of organics, oxidants and water, Atmos. Chem. Phys., 12, 2777–2794, doi:10.5194/acp-12-2777-2012, 2012.

Shiraiwa, M., Zuend, A., Bertram, A. K., and Seinfeld, J. H.: Gas-particle partitioning of atmospheric aerosols: interplay of physical mixing and morphology, Phys. Chem. Chem. Phys., 15, 11 441–11 453, doi:10.1039/c3cp51595h, 2013.

Vaden, T. D., Imre, D., Beránek, J., Shrivastava, M., and Zelenyuk, A.: Evaporation kinetics and phase of laboratory and ambient secondary organic aerosol, Proc. Natl. Acad. Sci., 108, 2190–2195, doi:10.1073/pnas.1013391108, 2011.

Verwer, J. G., Spee, E. J., Bloom, J. G., and Hundsdorfer, W.: A second-order rosenbrock method applied to photochemical dispersion problems, SIAM J. Sci. Comput., 20, 1456–1480, doi:10.1137/S1064827597326651, 1999.

Virtanen, A., Joutsensaari, J., Koop, T., Kannosto, J., YliPirilä, P., Leskinen, J., Mäkelä, J. M.,

49

Holopainen, J. K., Pöschl, U., Kulmala, M., Worsnop, D. R., and Laaksonen, A.: An amorphous solid state of biogenic secondary organic aerosol particles, Nature, 467, 824–827, doi:10.1038/nature09455, 2010.

Wang, Y., Sartelet, K., Bocquet, M., and Chazette, P.: Modelling and assimilation of lidar signals over Greater Paris during the MEGAPOLI summer campaign, Atmos. Chem. Phys., accepted for publication, 2014.

WHO: Health Aspects of Air Pollution with Particulate Matter, Ozone and Nitrogen Dioxide, Tech. rep., WHO EUR/03/5042688, 2003.

Yu, S., Bhave, P. V., Dennis, R. L., and Marthur, R.: Seasonal and regional variations of primary and secondary organic aerosols over the Continental United States: Semi-empirical estimates and model evaluation, Environ. Sci. Technol., 41, 4690–4697, doi:10.1021/es061535g, 2007.

Zhang, Q., Jimenez, J. L., Canagaratna, M. R., Allan, J. D., Coe, H., Ulbrich, I., Alfarra, M. R., Takami, A., Middlebrook, A. M., Sun, Y. L., Dzepina, K., Dunlea, E., Docherty, K., De-Carlo, P. F., Salcedo, D., Onasch, T., Jayne, J. T., Miyoshi, T., Shimono, A., Hatakeyama, S., Takegawa, N., Kondo, Y., Schneider, J., Drewnick, F., Borrmann, S., Weimer, S., Demerjian, K., Williams, P., Bower, K., Bahreini, R., Cottrell, L., Griffin, R. J., Rautiainen, J., Sun, J. Y., Zhang, Y. M., and Worsnop, D. R.: Ubiquity and dominance of oxygenated species in organic aerosols in anthropogenically-influence Northern Hemisphere mildlatitudes, Geophys. Res. Lett., 34, L13 801, doi:10.1029/2007GL029979, 2007.

Zuend, A. and Seinfeld, J. H.: Modeling the gas-particle partitioning of secondary organic aerosol: the importance of liquid-liquid phase separation, Atmos. Chem. Phys., 12, 3857–3882, doi:10.5194/acp-12-3857-2012, 2012.

Zuend, A., Marcolli, C., Luo, B. P., and Peter, T.: A thermodynamic model of mixed organic-inorganic aerosols to predict activity coefficients, Atmos. Chem. Phys., 8, 45594593, doi:10.5194/acp-8-4559-2008, 2008.

Zuend, A., Marcolli, C., Peter, T., and Seinfeld, J. H.: Computation of liquid-liquid equilibria and phase stabilities: implications for RH-dependent gas/particle partitioning of organic-inorganic aerosols, Atmos. Chem. Phys., 10, 7795–7820, doi:doi:10.5194/acpd-10-12497-2010, 2010.

Zuend, A., Marcolli, C., Booth, A. M., Lienhard, D. M., Soonsin, V., Krieger, U. K., Topping, D. O., McFiggans, G., Peter, T., and Seinfeld, J. H.: New and extended parameterization of the thermodynamic model AIOMFAC: calculation of activity coefficients for organic-inorganic mixtures containing carboxyl, hydroxyl, carbonyl, ether, ester, alkenyl, alkyl, and aromatic functional groups, Atmos. Chem. Phys., 11, 9155–9206, doi:10.5194/acp-11-9155-2011, 2011.
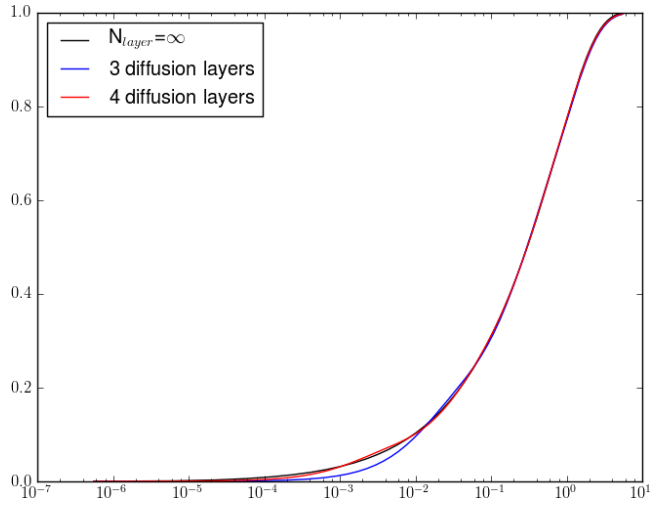
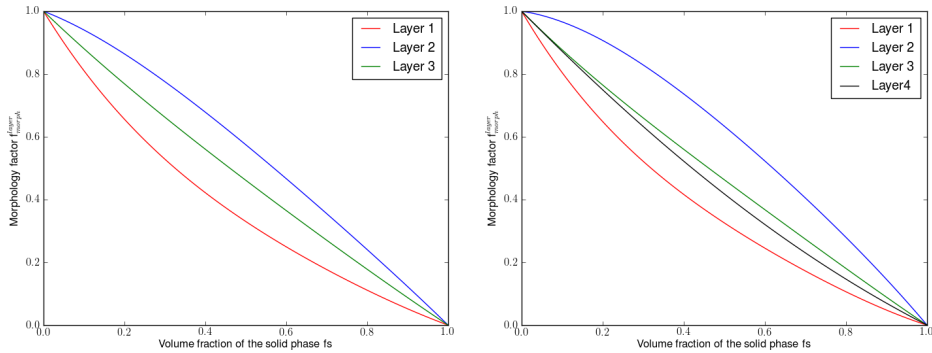**Fig. 1.** Evolution of the ratio $A_p(t)/A_{eq}$ as a function of the ratio t/τ_{dif}.

Fig. 2. Morphology factors as a function of the volume fraction of the solid phase (Layer 1 corresponds to the layer near the solid core of the particle and Layer 3 to the layer near the interface) for 3 diffusion layers (left) and 4 diffusion layers (right).
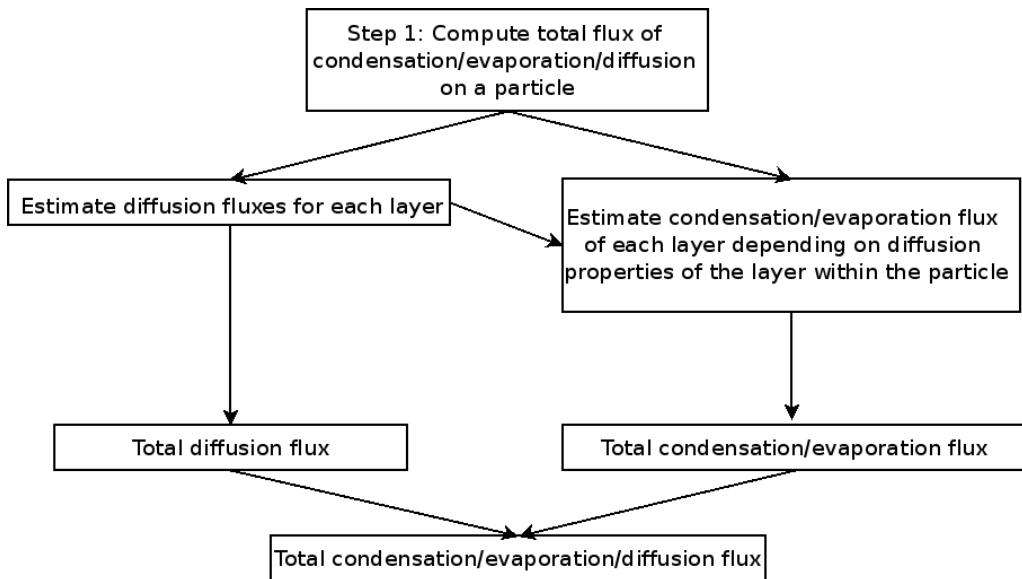
Fig. 3. Diagram of the first step of the algorithm to compute evaporation/condensation/diffusion fluxes.
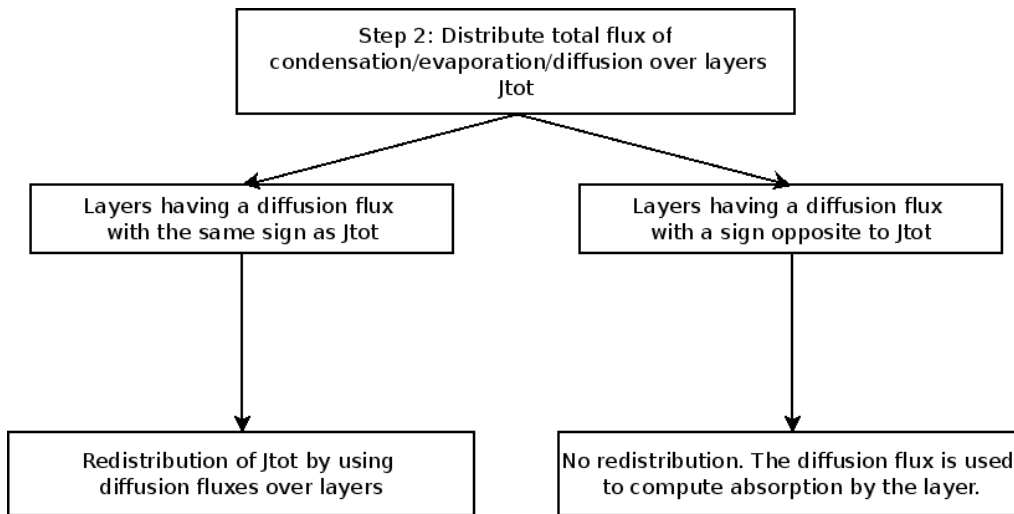
Fig. 4. Diagram of the second step of the algorithm to compute evaporation/condensation/diffusion fluxes.

	While the system has not converged (or has not reached a maximum number of iterations):
1.	$n = 1$
2.	factor = $1/n$
3.	Compute the new estimation of the concentrations $A_{p,i,new}^{bin,layer,phase}$ according to Eq. 81.
4.	Errors = $(A_{p,i,new}^{bin,layer,phase} - A_{p,i}^{bin,layer,phase})/ A_{p,i}^{bin,layer,phase}$
5.	$A_{p,i}^{bin,layer,phase}$ = factor $\times$ $A_{p,i,new}^{bin,layer,phase}$ + (1 - factor) $\times$ $A_{p,i}^{bin,layer,phase}$
6.	Compute $M_{o}^{bin,layer,phase}$
7.	If the system can not converge (the system is in a situation where relative errors on concentrations between two steps does not change or return to old values), $n = n + 1$
8.	If the system has not converged (relative errors on concentrations between two steps are too high), return to step 2

Table 1. Algorithm to compute the partitioning of compounds at equilibrium in the dynamic approach.
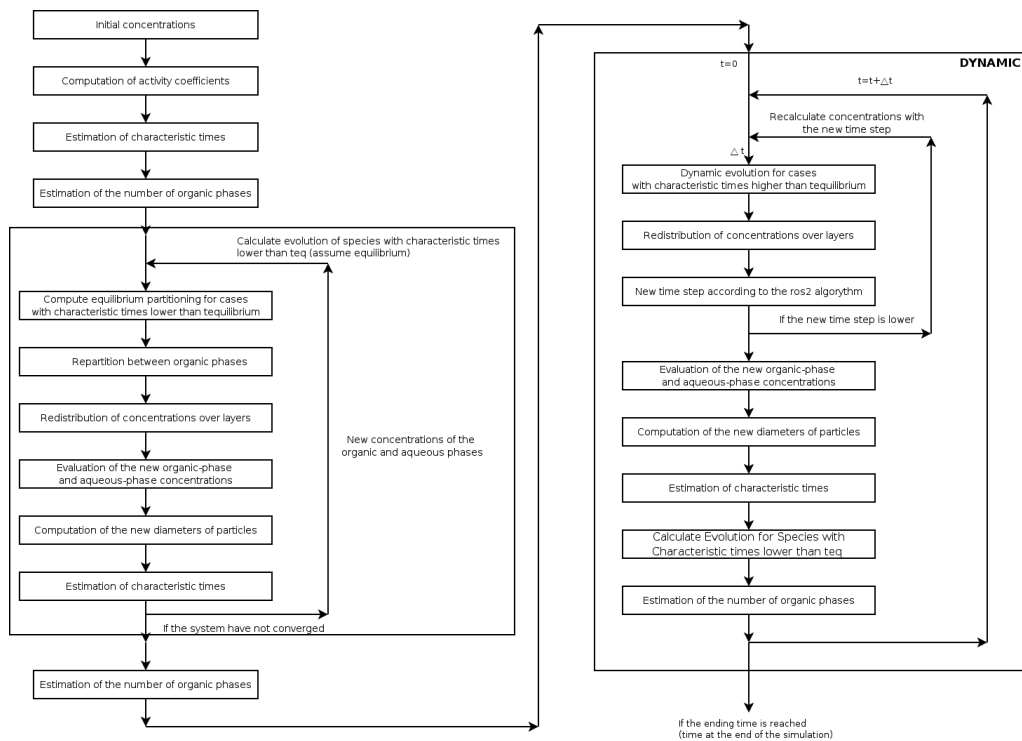
Fig. 5. Diagram of the method used to compute the evolution of concentrations.
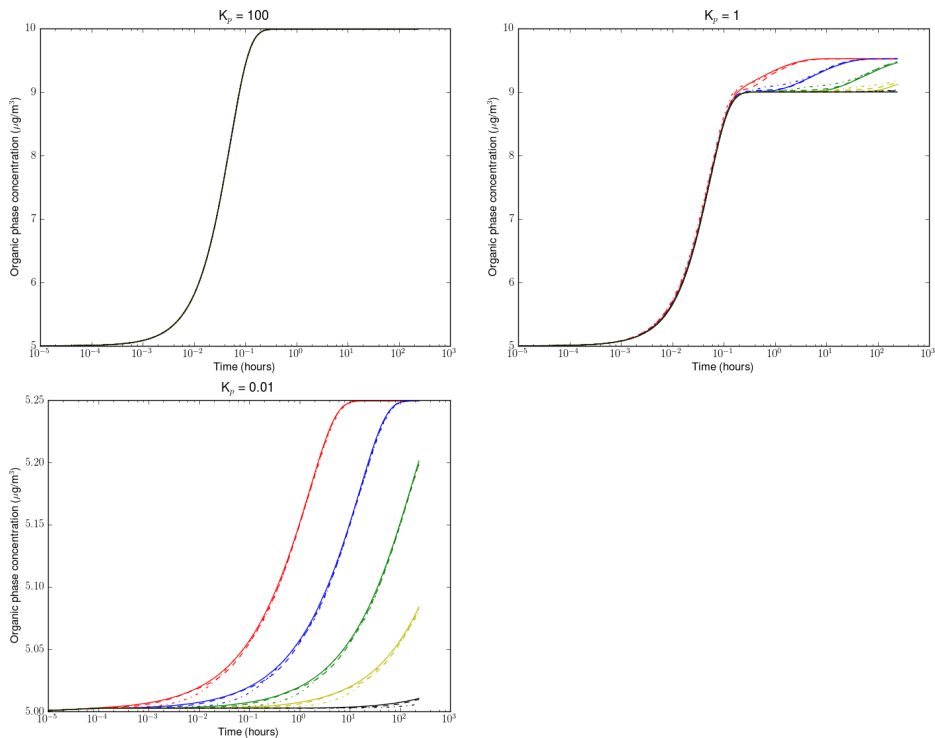
Fig. 6. Comparison between the explicit representation (plain lines) and the implicit representation for $N_{layer} = 5$ (– line) and $N_{layer} = 4$ (-. line) for several organic-phase diffusivity: $D_{org}=10^{-19}$ m^2/s (red), $D_{org}=10^{-20}$ m^2/s (blue), $D_{org}=10^{-21}$ m^2/s (green), $D_{org}=10^{-22}$ m^2/s (yellow) and $D_{org}=10^{-24}$ m^2/s (black) for a compound (with a partitioning coefficient of 100, 1 and 0.01 μg m^{-3}) condensing on 5 μg m^{-3} of non-volatile organic compounds.
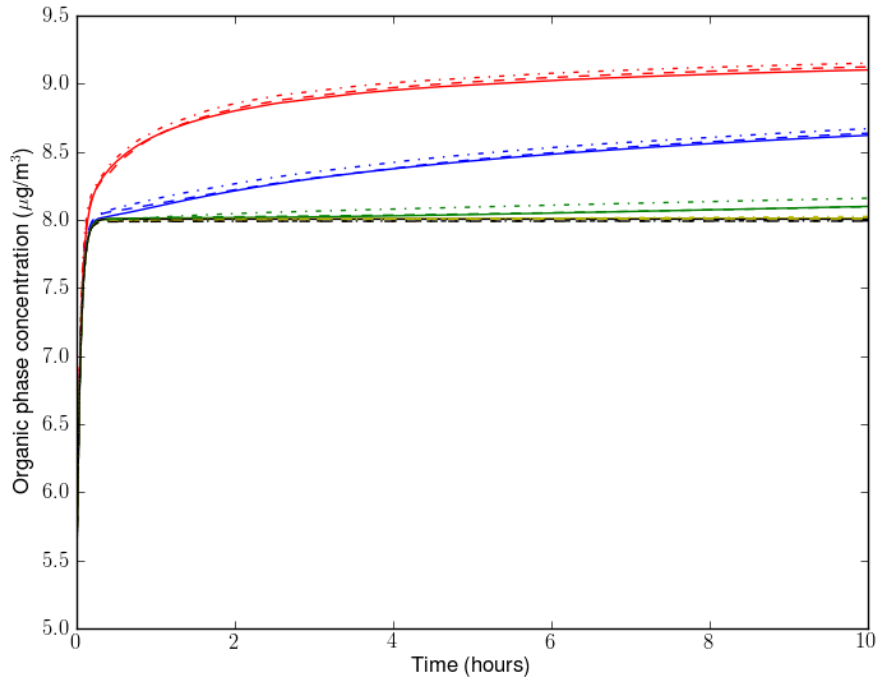
Fig. 7. Comparison between the explicit representation (plain lines) and the implicit representation for $N_{layer} = 5$ (– line) and $N_{layer} = 4$ (-. line) for several organic-phase diffusivity: $D_{org} = 10^{-19}$ m^2/s (red), $D_{org} = 10^{-20}$ m^2/s (blue), $D_{org} = 10^{-21}$ m^2/s (green), $D_{org} = 10^{-22}$ m^2/s (yellow) and $D_{org} = 10^{-24}$ m^2/s (black) for the compounds from biogenic test case (with an initial concentrations inside the particle equal to 10% of the concentration at equilibrium) condensing on 5 μg m^{-3} of non-volatile organic compounds at RH=30%. Ideality is assumed.

Fig. 8. Evolution of concentrations in organic phases for the biogenic case at various humidities, with initial concentrations equal to one tenth the concentrations at equilibrium and 5 μg m^{-3} of non-volatile compounds for N$_{layer}$=5 s (plain lines) and N$_{layer}$=4 (dashed lines) for several organic-phase diffusivity: D$_{org}$=10^{-19} m^2/s (red), D$_{org}$=10^{-20} m^2/s (blue), D$_{org}$=10^{-21} m^2/s (green), D$_{org}$=10^{-22} m^2/s (yellow) and D$_{org}$=10^{-24} m^2/s (black).

57
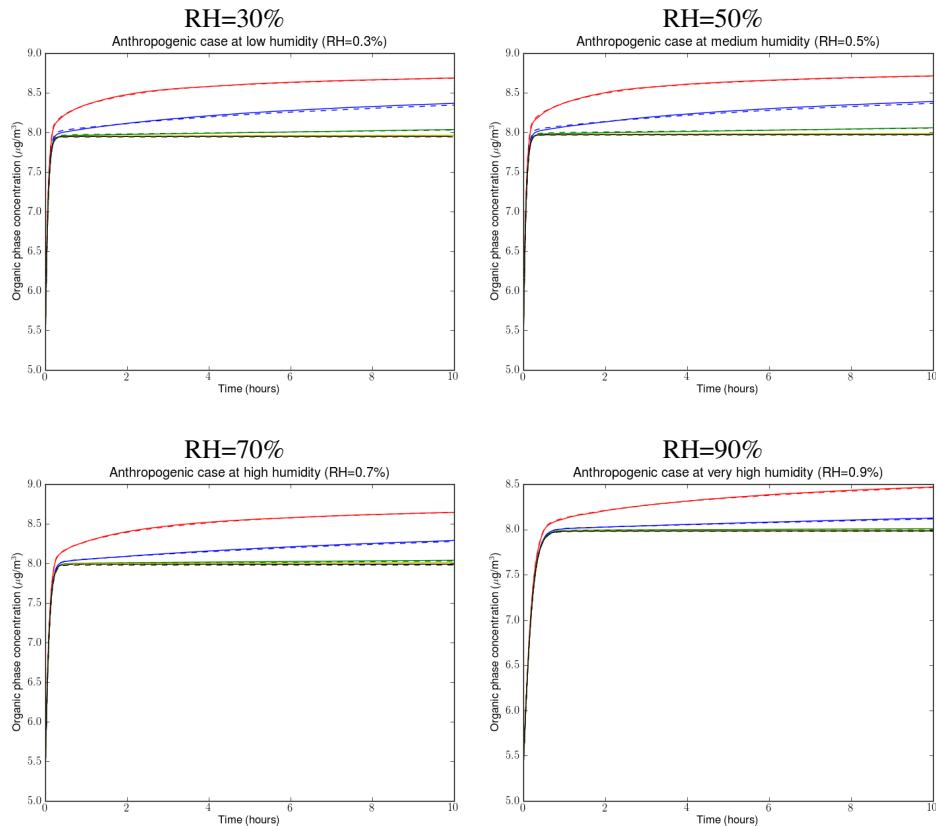
Fig. 9. Evolution of concentrations in organic phases for the anthropogenic case at various humidities, with initial concentrations equal to one tenth the concentrations at equilibrium and 5 μg m^{-3} of non-volatile compounds for N_{layer}=5 s (plain lines) and N_{layer}=4 (dashed lines) for several organic-phase diffusivity: D_{org}=10^{-19} m^2/s (red), D_{org}=10^{-20} m^2/s (blue) , D_{org}=10^{-21} m^2/s (green), D_{org}=10^{-22} m^2/s (yellow) and D_{org}=10^{-24} m^2/s (black).
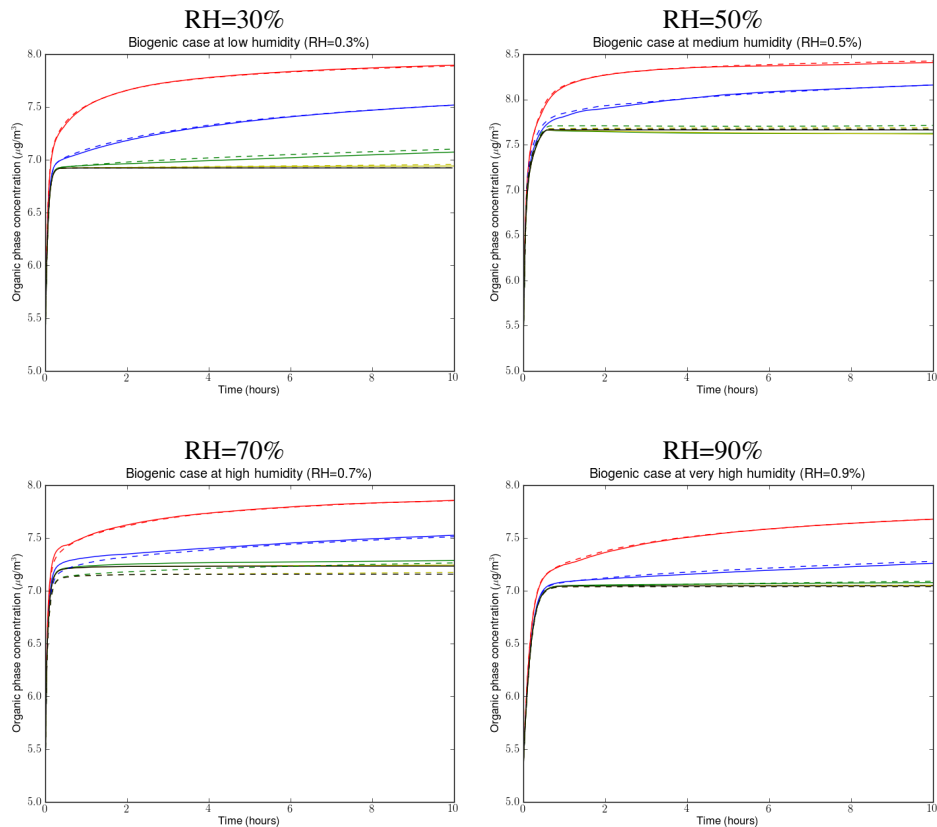
Fig. 10. Evolution of concentrations in the aqueous phase for the biogenic case at various humidities, with initial concentrations equal to tenth the concentrations at equilibrium and 5 μg m^{-3} of non-volatile compounds for N_{layer}=5 s (plain lines) and N_{layer}=4 (dashed lines) for several organic-phase diffusivity: D_{org}=10^{-19} m^2/s (red), D_{org}=10^{-20} m^2/s (blue) , D_{org}=10^{-21} m^2/s (green), D_{org}=10^{-22} m^2/s (yellow) and D_{org}=10^{-24} m^2/s (black).

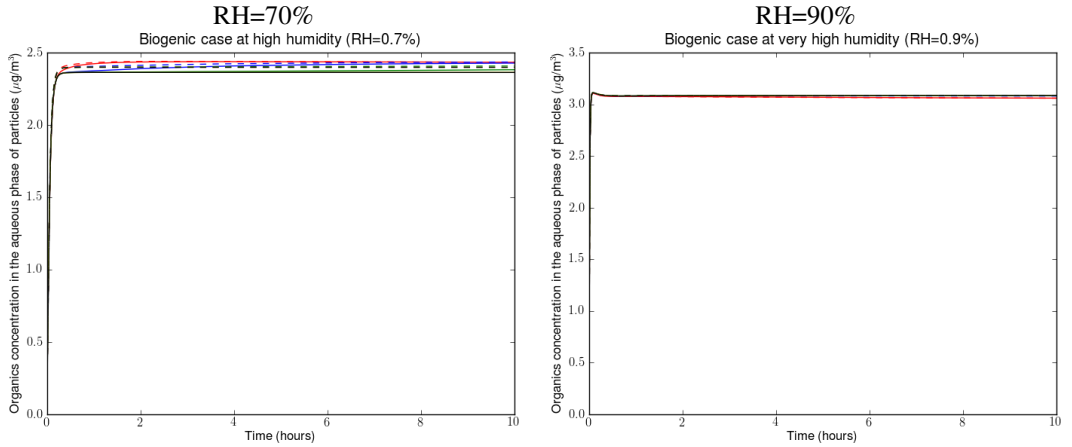|	layer	A_{layer}	B_{layer}	C_{layer}	D_{layer}
	1	0.5294	-1.6357	2.2070	-2.1006
3 diffusion layers	2	-0.3171	0.8786	-1.0613	-0.5002
	3	0.1375	-0.3707	0.4698	-1.2367
	1	0.6880	-1.9700	2.4440	-2.1617
4 diffusion layers	2	0.1210	0.3567	-1.1614	-0.2698
	3	0.3155	-0.7826	0.7822	-1.3147
	4	-0.1364	0.2046	0.3282	-1.3954

Table 2. Polynomial parameters for Eq. (41).
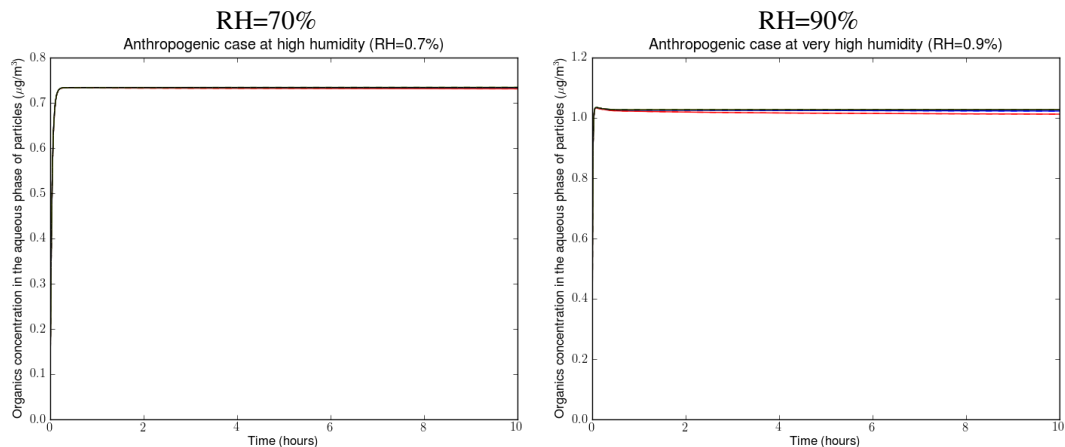
Fig. 11. Evolution of concentrations in the aqueous phase for the anthropogenic case at various humidities, with initial concentrations equal to tenth the concentrations at equilibrium and 5 μg m^{-3} of non-volatile compounds for N_{layer}=5 s (plain lines) and N_{layer}=4 (dashed lines) for several organic-phase diffusivity: D_{org}=10^{-19} m^2/s (red), D_{org}=10^{-20} m^2/s (blue) , D_{org}=10^{-21} m^2/s (green), D_{org}=10^{-22} m^2/s (yellow) and D_{org}=10^{-24} m^2/s (black).

1.	For each bin: If the new mass of organics $M_o^{bin,new}=\sum_{layer}\sum_{phase}M_o^{bin,layer,phase,new}$ is higher than the mass at previous iteration or time step (before adding new compounds) $M_o^{bin,old}$, the redistribution is done from the interface layer to the center of the particle: from ilayer=N_{layer} to 2, ilayer2=ilayer-1. If the new mass of organics $M_o^{bin,new}=\sum_{layer}\sum_{phase}M_o^{bin,layer,phase,new}$ is lower than the mass at previous iteration or time step (before adding new compounds) $M_o^{bin,old}$, the redistribution is done from the center of the particle to the interface layer: from ilayer=1 to N_{layer}-1, ilayer2=ilayer+1:
2.1	If the mass of the layer increased:
2.1.1	Mass to be redistributed: $\Delta M=M_o^{bin,layer,new}-\alpha_{layer}*M_o^{bin,new}$
2.1.2	Fraction of concentrations to redistribute: $f=\frac{\Delta M}{M_o^{bin,layer,new}}$
2.1.3	The exceeding mass of the layer is transmitted to the next layer (ilayer 2): $A_p^{bin,layer2,phase}=A_p^{bin,layer2,phase}+f*A_p^{bin,layer,phase}$ $A_p^{bin,layer,phase}=(1\text{-}f)*A_p^{bin,layer,phase}$
3.1	If the mass of the layer decreased:
3.1.1	Mass to be redistributed: $\Delta M=\alpha_{layer}*M_o^{bin,new}-M_o^{bin,layer,new}$
3.1.2	Fraction of concentrations to redistribute from the next layer (ilayer2): $f=\frac{\Delta M}{M_o^{bin,layer2,new}}$
3.1.3	The missing mass of the layer is taken from the next layer (ilayer 2): $A_p^{bin,layer,phase}=A_p^{bin,layer,phase}+f*A_p^{bin,layer2,phase}$ $A_p^{bin,layer2,phase}=(1\text{-}f)*A_p^{bin,layer2,phase}$

Table 3. Algorithm to compute the redistribution of compounds between layers.

Table 4. Description of the H^{2}O surrogate SOA species. Volatility is very low for compounds with $K_p{>}100$, low for compounds with $100 \geq K_p{>}1$, medium for compounds with $1 \geq K_p{>}0.1$, high for compounds with $0.1 \geq K_p{>}0.01$ and very high for compounds with $K_p \leq 0.01$. A and B species are respectively hydrophilic and hydrophobic compounds.

Surrogate	Type	Precursors	Conditions of formation	Volatility
BiMT	A	isoprene	Oxydation by OH (low NO$_x$)	high
BiPER	A	isoprene	Oxydation by OH (low NO$_x$)	high
BiDER	A	isoprene	Oxydation by OH (low NO$_x$)	medium
BiMGA	A	isoprene	Oxydation by OH (high NO$_x$)	medium
BiNGA	B	isoprene	Oxydation by OH (high NO$_x$)	medium
BiNIT3	B	isoprene	Oxydation by NO$_3$	high
BiA0D	A	monoterpenes	Oxydation by OH and O$_3$	very low if the aqueous aerosol is acidic
BiA1D	A	monoterpenes	Oxydation by OH and O$_3$	medium
BiA2D	A	monoterpenes	Oxydation by OH and O$_3$	medium
BiNIT	B	monoterpenes	Oxydation by NO$_3$	high
BiBlP	B	sesquiterpenes	Oxydation by OH	very low
BiBmP	B	sesquiterpenes	Oxydation by OH	medium
AnBlP	B	aromatics	Oxydation by OH (low NO$_x$)	low
AnBmP	B	aromatics	Oxydation by OH (low NO$_x$)	high
AnClP	B	aromatics	Oxydation by OH (high NO$_x$)	non-volatile
POAlP	B	-	Primary SVOC	low
POAmP	B	-	Primary SVOC	high
POAhP	B	-	Primary SVOC	very high
SOAlP	B	POAlP	Oxydation by OH	very low
SOAmP	B	POAmP	Oxydation by OH	low
SOAhP	B	POAhP	Oxydation by OH	high

Compounds	Concentration (μg m^{-3}) Biogenic test case at T = 295 K	Concentration (μg m^{-3}) Anthropogenic test case at T = 293 K
BiA2D	0.07	0.02
BiA1D	0.74	0.20
BiA0D	1.02	0.58
BiPER	1.46	0.17
BiDER	0.45	0.06
BiMGA	0.25	0.05
AnBlP	0.03	0.05
AnBmP	0.27	0.32
BiBlP	0.09	0.03
BiBmP	0.22	0.07
AnClP	0.07	0.03
BiNGA	0.21	0.05
BiNIT3	0.13	0.02
BiNIT	0.44	0.13
POAlP	0.10	0.71
POAmP	0.02	0.69
POAhP	0.03	0.91
SOAlP	0.36	0.65
SOAmP	0.70	1.35
SOAhP	1.72	2.51
H_2SO_4	1.70	1.44
HNO_3	1.83	5.07
NH_3	1.07	1.77

Table 5. Conditions of the test cases.

	Biogenic test case		Anthropogenic test cases	
	A_p (μg m^{-3})	A_{aq} (μg m^{-3})	A_p (μg m^{-3})	A_{aq} (μg m^{-3})
monoterpenes	0.83	1.01	0.22	0.58
sesquiterpenes	0.28	0.0	0.10	0.0
isoprene	0.89	0.70	0.13	0.12
aromatics	0.09	0.05	0.09	0.04
primary SVOC	0.09	0	0.70	0.0
oxidized primary SVOC	1.22	0	2.28	0.0
Water	0.66	1.86	0.48	2.68

Table 6. Concentrations of organic aerosols formed for each precursor for both test cases at RH=70% if ideality is assumed.

	Biogenic test case		Anthropogenic test cases	
	A_p (μg m^{-3})	A_{aq} (μg m^{-3})	A_p (μg m^{-3})	A_{aq} (μg m^{-3})
monoterpenes	0.44	1.10	0.14	0.55
sesquiterpenes	0.19	0.0	0.08	0.0
isoprene	0.18	1.24	0.02	0.13
aromatics	0.09	0.16	0.07	0.01
primary SVOC	0.08	0	0.68	0.0
oxidized primary SVOC	1.04	0	2.18	0.0
Water	0.06	1.05	0.06	2.75

Table 7. Concentrations of organic aerosols formed for each precursor for both test cases at RH=70% if non-ideality is assumed (with short-range, medium-range and long-range interactions).

Compound	Fraction of the compound in the organic phase (in %)	
	Biogenic test case	Anthropogenic test case
BiA2D	75	99
BiA1D	89	100
BiA0D	0	0
BiPER	2	3
BiDER	2	1
BiMGA	80	59
AnBlP	75	100
AnBmP	6	50
BiBlP	99	100
BiBmP	100	100
AnClP	100	100
BiNGA	98	99
BiNIT3	70	97
BiNIT	97	100

Table 8. Distributions of surrogate organic compounds between the aqueous phase and the organic phase.

Compound	Without phase separation	With phase separation		
	A_p	1st phase	2nd phase	all phases
BiA2D	0.042	0.037	0.005	0.042
BiA1D	0.322	0.299	0.021	0.320
BiA0D	0.001	0.0	0.001	0.0
BiPER	0.031	0.026	0.030	0.056
BiDER	0.015	0.011	0.048	0.059
BiMGA	0.027	0.020	0.040	0.060
AnBlP	0.012	0.011	0.001	0.012
AnBmP	0.012	0.010	0.010	0.020
BiBlP	0.092	0.091	0.001	0.092
BiBmP	0.098	0.096	0.0	0.096
AnClP	0.069	0.069	0.0	0.069
BiNGA	0.062	0.051	0.020	0.071
BiNIT3	0.010	0.010	0.001	0.011
BiNIT	0.043	0.041	0.001	0.042
POAlP	0.076	0.075	0.0	0.075
POAmP	0.001	0.0	0.0	0.0
POAhP	0.0	0.0	0.0	0.0
SOAlP	0.356	0.356	0.0	0.356
SOAmP	0.532	0.527	0.0	0.527
SOAhP	0.132	0.127	0.0	0.127
Water	0.020	0.018	0.012	0.030
Sum of organics	1.933	1.857	0.173	2.035

Table 9. Concentrations (in μg m^{-3}) with or without phase separation for the biogenic test case at RH=30%.

| Phenomena taken into account | | | | Time for | |
Coupled system	Short range interactions	Long and medium range interactions	Organic phase separation	Equilibrium approach	Dynamic approach
				1	400
X				1.4	800
	X			4.2	2400
X	X			18	4400
	X	X		7	2500
X	X	X		23	5400
	X	X	X	23	2600
X	X	X	X	79	66000

Table 10. Time necessary to solve the biogenic case at RH=70% (relative to the time necessary to solve the case with an uncoupled system with ideality) for different configurations of the model.